STRESS INTENSITY VALUES FOR PRENOTCHED AND PRECRACKED, PLAIN CONCRETE BEAMS

M. Fartash

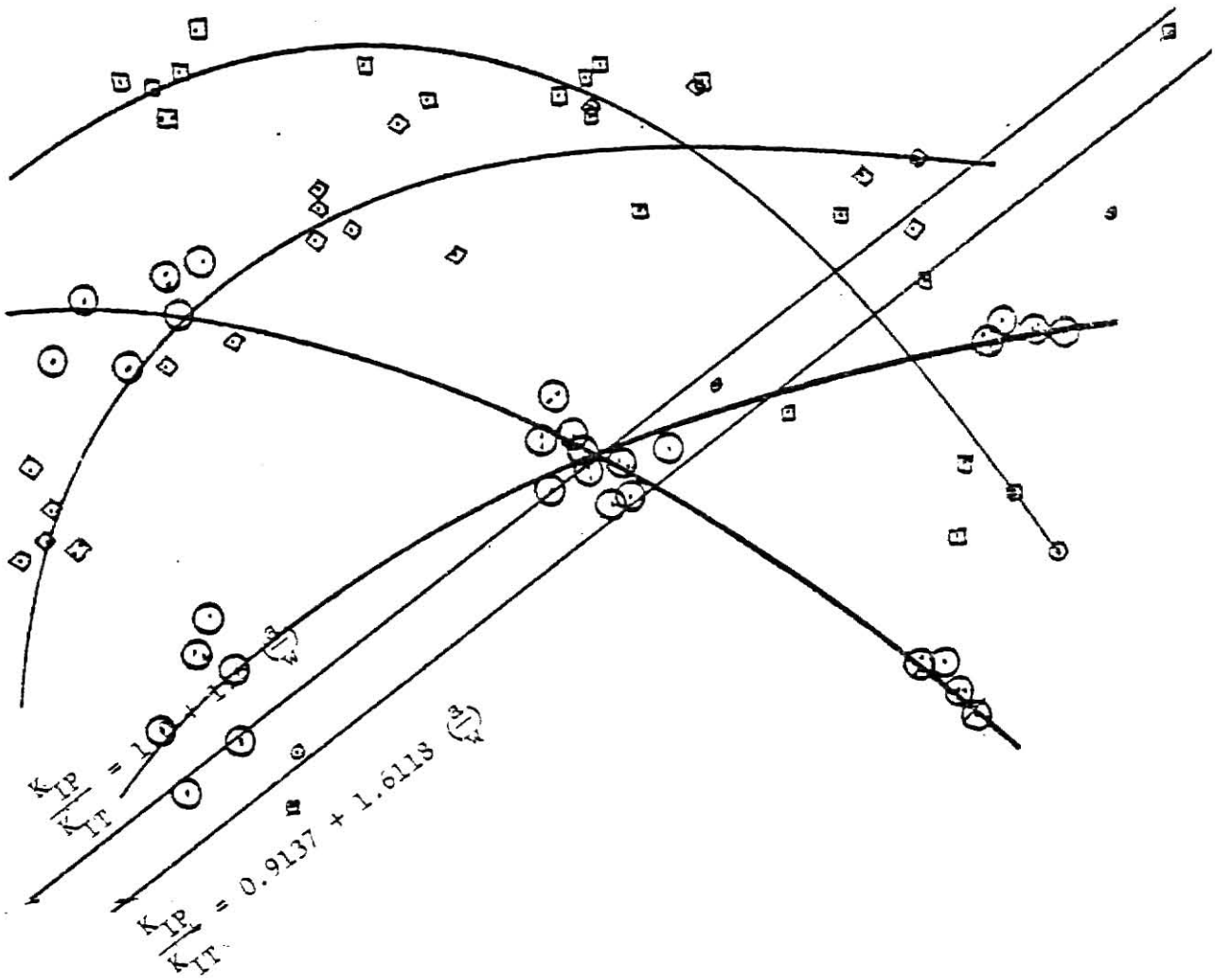

STRESS INTENSITY VALUES FOR PRENOTCHED AND PRECRACKED, PLAIN CONCRETE BEAMS

by

Mojtaba Fartash

B.S., University of Missouri-Columbia, 1979

A MASTER'S THESIS

submitted in partial fulfillment of the

requirements for the degree of

MASTER OF SCIENCE

Department of Civil Engineering

KANSAS STATE UNIVERSITY
Manhattan, Kansas

1981

Approved:

Major Professor

TABLE OF CONTENTS

THIS BOOK
CONTAINS
NUMEROUS PAGES
WITH ILLEGIBLE
PAGE NUMBERS
THAT ARE CUT OFF,
MISSING OR OF POOR
QUALITY TEXT.

THIS IS AS RECEIVED
FROM THE
CUSTOMER.

Acknowledgements

The author would like to express his appreciation to Dr. Stuart E. Swartz for his assistance and guidance in the writing and editing of this thesis. Further acknowledgement should be extended to my parents, Mr. and Mrs. Jalil Fartash, for their moral support. I would also like to thank Mr. Russell Gillespie, Civil Engineering Technician for assisting me in using the M.T.S. and other machines. Special thanks is given to Mrs. Peggy Selvidge and Mrs. Ruth Ashmore, Civil Engineering secretaries, for the typing of this thesis.

LIST OF TABLES

LIST OF FIGURES

LIST OF FIGURES (continued)

NOTATIONS

a - Crack Depth

c - Width of Beam

C MOD - Crack Mouth Opening Displacement

D - Diameter

K_I - Stress Intensity Value for Concrete Beams

K_{IP} - Stress Intensity Value for Precracked Beams

K_{IT} - Stress Intensity Value for Prenotched Beams

L - Length of Beam

P - Load

$P_{max.}$ - Maximum Load

W - Depth of Beam

σ_b - Net Bending Stress

Chapter 1

INTRODUCTION

A number of investigations directed toward measuring the fracture toughness of cementitious materials utilizing either notched or pre-cracked beam specimens is reported (6).

The most comprehensive work reported to date using "notched" specimens is that of Naus and Lott (4) in which effective fracture toughness was determined for concrete beams and related to various mix design parameters. The notches were formed using 0.003 in. (0.0762 mm.) thick teflon strips cast into the specimens and effective fracture toughness was determined by using the formula of Brown and Srawley (1).

On the other hand, tests performed on limestone beams by Schmidt (5) indicated that a crack cannot be adequately simulated by a notch for the purpose of measuring fracture toughness because of the closure phenomenon associated with natural cracks. This has been observed also in concrete (6).

Only recently has hardware been available that would allow cracks to be grown in a controlled manner in plain concrete beams subjected to bending. As described in References 3, 6, and 8 it is possible to pre-crack beams either statically or in fatigue in a controlled manner.

A series of experiments conducted to compare the behavior of beams with notches to those with natural cracks has recently been completed. A total of 42 beams with notches formed by casting teflon strips into the concrete was tested to failure. A companion series of 42 beams was statically precracked following the procedure described in Reference (3). The ranges of crack depth to beam depth varied from 0.3 to 0.7

(nominally). Two strengths of concrete were used with 3 in. x 4 in. x 15 in. (76.2 mm. x 101.60 mm. x 381.0 mm.) beams tested in three-point or four-point bending.

The results of this study reported herein indicate a linear correlation in stress-intensity (K_I) values obtained between notched and precracked beams as a function of a/w where a is the total crack depth and w is the depth of the beam.

In chapter two some other similar experiments have been reviewed; chapter three describes fully the experimental program. In chapter four, test results are discussed, while chapter five summarizes the report.

Chapter 2

LITERATURE REVIEW

Fracture toughness is a material property determined by evaluating the stress-intensity factor in an opening mode at the onset of rapid, unstable crack propagation (4).

The stress-intensity factor denotes the elastic stress and displacement fields in the region of the crack tip of a homogeneous material. When concrete is analyzed as a homogeneous material an "effective" fracture toughness is obtained (4).

Previous investigations in determining the stress intensity values for concrete beams have been somewhat limited. Earlier work done that closely approximates the present experiment was performed by Naus and Lott (4) in which the "effective" fracture toughness of several pastes, mortars, and concretes was determined by flexural tests of specimens containing flaws of various depths cast at the center of the tensile surface. The flaw was formed with a strip of teflon-coated fiberglass cloth with a thickness of 0.003 in. (0.0762 mm.). The nominal flaw depths used were: 0.25 in (6.35 mm.), 0.5 in. (12.7 mm.), and 1.0 in. (25.4 mm.) for the paste and mortar series, and 0.5 in. (12.7 mm.), 1.0 in. (25.4 mm.), and 1.5 in. (38.1 mm.) for the concrete series. Variation in the nominal dimensions occured during fabrication, and actual dimensions of the specimens were measured after testing. Materials used in the Naus and Lott experiment were type I portland cement, fine-graded Wabash river sand and two types of gravel: a Wabash river gravel and a locally-obtained crushed limestone. Nominal dimensions of the flexural specimens for the paste and mortar series were 2 x 2 x 14 in. (51 x 51 x 305 mm), and the nominal dimensions of the flexural specimens for concrete series were 4 x 4 x 12 in. (102 x 102 x 305 mm).

The effective fracture toughness (critical stress intensity factor) is the determination of the stress intensity factor at maximum moment.

Their result included the following:

1. The effective fracture toughness decreased with increasing water-cement ratio for paste and mortar series. There was no apparent effect of varying the water-cement ratio on effective fracture toughness for the concrete series.
2. Increasing the air content decreased the effective fracture toughness for the paste, mortar, and concrete series.
3. In the paste, mortar, and concrete series there was an increase in effective fracture toughness with age.
4. There was an increase in effective fracture toughness with increasing sand-cement ratio for the mortar series; however, for the concrete series there was a decrease in effective fracture toughness with increasing sand-cement ratio.
5. The effective fracture toughness of the concrete series increased with an increase in maximum size of coarse aggregate.
6. Increasing the gravel-cement ratio increased the effective fracture toughness of concrete.
7. The effective fracture toughness of the concrete series cast with a river gravel coarse aggregate was lower than the effective fracture toughness of a concrete series cast with a crushed limestone coarse aggregate for ages of three days and six days; however, at ages of twenty-eight days and ninety days the difference in their effective fracture toughness was small compared to that prior to twenty-eight days.

Another experiment was reported by Hillemeier and Hilsdorf (2). Materials used in this experiment were German cement PZ350F with a water-cement ratio of 0.40. All tests were conducted at a specimen age of seven days. Two types of rocks used for the concrete aggregate were quartz and marble. They used a "compact tension specimen" or CT-Specimen to determine the fracture toughness of the material.

They define fracture toughness to be the stress-intensity associated with the start of crack extension.

Results they obtained were as follows:

1. Hardened cement paste is a notch---sensitive material.
2. Wedge-loaded compact-tension specimens are suitable to determine fracture mechanics characteristics of hardened cement pastes and hardened cement paste-aggregate interfaces since they allow the controlled development of crack growth in a simple manner.
3. As a crack grows in the hardened cement paste specimen from an initial notch the fracture toughness for further crack growth decreases with increasing crack length and approaches a constant value.
4. This constant value is independent of the initial notch depth and may be considered the true fracture toughness of hardened cement paste for the growth of a single crack.
5. Similar behavior has been observed for quartz-hardened cement paste interfaces. However, the fracture toughness of such interfaces is considerably lower than the corresponding value for hardened cement paste.
6. The fracture toughness values of marble and quartz are approximately an order of magnitude larger than those of hardened cement paste with a water cement ratio of 0.4.

7. The addition of a polymer dispersion led to a substantial increase of the fracture toughness of quartz-hardened cement paste interfaces, whereas, the fracture toughness of the hardened cement paste matrix decreased.
8. The ductility of model concretes tested in flexure primarily depended on the fracture toughness of the aggregate-hardened cement paste interfaces. Modifications of a hardened cement paste of a given water-cement ration by various additions had less effect on concrete flexural ductility.

An experiment was reported by Swartz, Huang, and Hu (8). As a part of an ongoing experimental/analytical research effort to evaluate the feasibility of a test method for fracture toughness of concrete, forty-eight plain concrete beams were tested in bending to failure. All beams were notched and then precracked to different crack length/depth ratios prior to loading to failure. The precracking was done using an electro-hydrodynamic materials testing system and displacement control.

The beams which were cracked in fatigue were subjected to one million cycles of sinusoidal loading of $4H_Z$. After the cycling was complete on a beam, the crack depth was determined using a compliance calibration technique (6), following which the beam was loaded to failure. A load versus crack-mouth-opening-displacement trace was plotted during this final load run.

For each beam tested in fatigue, a companion beam was precracked "statically" by loading in repeated cycles until the crack depth, as measured by compliance calibration, matched that of the fatigued specimen.

The studies were made on two different beam sizes in three and four-point bending with two different mix designs. They define effective

fracture toughness to be the stress intensity at the end of the crack associated with the load at the onset of unstable crack growth. This load is defined to be the ultimate load obtained in the test for a sufficiently long crack.

Results they obtained were as follows:

1. It is possible to precrack plain concrete beams to a desired depth with reasonable accuracy using commercially available testing equipment. Furthermore, this can be accomplished fairly easily by an operator with a nominal amount of training.
2. For concrete, static precracking prior to loading to failure to determine fracture thoughness is acceptable, even for fatigue loading cases.
3. The writers feel the only valid approach to determining fracture toughness in concrete is by using natural cracks, i.e., notches or inserts do not adequately model a crack.
4. Using precracked specimens, beams with depths as small as four inches (102 mm.) exhibit notch-sensitivity. The results for beams this size were essentially the same as for the larger beams with depth of eight inches (204 mm.).
5. More consistent results are obtained using 4-point bending. The reason for this may be due to the absence of a shear force at the location of the crack. It is recommended testing be done in 4-point bending. It is also recommended the supports be free to roll--instead of sliding.
6. Effective fracture toughness is clearly related to strength of concrete. This should be considered in the development of design/application formulas.

Chapter 3

EXPERIMENTAL PROGRAM

3.1 Test Specimens - one size of beam was constructed, Fig. 3.1, with the following dimensions:

W = 4 in. (101.6 mm.)
L = 15 in. (381.0 mm.)
C = 3 in. (76.2 mm.)

Two mix designs were used as given in table 3.1. The nominal strengths were 3200 psi (22.07 MPa) for mix A and 6700 psi (46.21 MPa) for mix B. The cylinder strengths in compression were measured during a given series of tests.

A total of ninety-six beams were made, forty-eight of each mix in three test series. In each test series two beams were used for compliance calibration and the rest were tested; thus a total of eighty-four beams were tested. These eighty-four beams were divided into six batches, identified by 1-A, 2-A, 3-A, 1-B, 2-B, and 3-B. The letters A and B represent the mix type and the numbers 1, 2, and 3 represent batches with different crack lengths. Batch 1-A had sixteen beams, two used for the compliance calibration, and seven with a teflon insert, 0.003 in. (0.0762 mm.) thick with a depth of 1.2 in. (30.48 mm.). The other seven were plain beams. Batches 2-A, and 3-A were similar to 1-A except that the depth of teflon was 2.0 in. (50.8 mm.) and 2.8 in. (71.12 mm.) respectively. These beams were tested in three-point bending. Batches 1-B, 2-B, and 3-B were the same as 1-A, 2-A, and 3-A except for higher strength concrete and type of applied load (four-point bending). The seven beams in each batch that were cut with a saw to a depth of about 0.4 in. (10.16 mm.) and then tested.

A special way of inserting the teflon into the concrete mold was used. The size of each mold, back to back, was 17 in. x 17.5 in. (431.8 mm. x 444.5 mm.). Each could hold four beams. Two plates were made, 18 in. x 3 in. x 1/4 in. (457.2 mm. x 76.20 mm. x 6.35 mm.), four angles were cut, 3 in. x 4 in. (76.2 mm. x 101.6 mm.), with a length of 6 in. (152.4 mm.). These angles were bolted to plates as shown in Figs. 3.2 and 3.3. For each size of teflon that was used, a type of V-shape aluminum plates was constructed to hold the teflon inside the mold. After concrete was poured the V-shape aluminum plates were removed carefully. After removing the plates and aluminum plates, beams with teflon insert are shown in Fig. 3.4.

Table 3.1 Mix Design

	Mix A	Mix B
water/cement	0.78	0.50
cement type	I	I
% sand (wt.)	31	31
sand dry Rodded unit wt.	106 pcf (16.63 kN/m^3)	106 pcf (16.63 kN/m^3)
S. G. Sand	2.62	2.62
Sand Moisture Content	0.50%	0.50%
Sand Fineness Modulus	3.35	3.35
% coarse Aggregate (wt.)	45	45
Aggregate dry Rodded unit wt.	94.5 pcf (14.82 kN/m^3)	94.5 pcf (14.82 kN/m^3)
S. G. Aggregate	2.59	2.59
Maximum Size Aggregate	0.5 in. (12.7 mm.)	0.5 in. (12.7 mm.)
Aggregate Moisture Content	0.3%	0.3%
Aggregate Fineness Modulus	6.41	6.41
Sand/Aggregate	0.69	0.69
Air Content	2.8%	3.2%
Slump	6.5 in. (165.1 mm.)	0.5 in. (12.7 mm.)
unit wt. of concrete	141.8 pcf (22.24 kN/m^3)	148.4 pcf (23.28 kN/m^3)

3.2 Test set up and Equipment

The test set ups for load application in 3 point and 4 point bending are shown schematically in Fig. 3.1. The actual support used initially for 3 point bending is reported elsewhere (6). The 4 point bending set up for these beams utilized a spreader beam to apply the two loads which were 5.5 in. (139.7 mm.) apart. The new arrangement is shown in Figs. 3.5 and 3.6 and is comprised of two steel blocks 6 in. (152.4 mm.) x 4 in. (101.6 mm.) x 3.6 in. (91.44 mm.) with notches to hold 2 in. (50.8 mm.) dia. steel rollers. These blocks are bolted to a 0.5 in. (12.7 mm.) thick steel plate as shown in Fig. 3.6.

All testing was done with an electro-hydraulic materials testing system. Crack-mouth-opening displacements (CMOD) were measured using a commercially available displacement transducer (MTS 632.05B-60) that has a maximum sensitivity of $\pm$ 0.002 in. ($\pm$0.0508 mm.) Per10-V full scale output.

3.3 Test Procedure

All crack length measurements were made using the compliance procedure described fully in Reference 6. Half of the tested beams were notched initially by a saw cut about 0.13 in. (3.3 mm.) wide with a depth of 0.4-0.45 in. (10.16-11.43 mm.). The other beams were "pre-notched" with teflon. The only purpose of the saw cut in the plain beams was to ensure the crack would start at midspan.

Using the compliance method and after the calibration curves for crack length had been obtained, the following procedures were used.

Prenotched with teflon and loaded to failure

1. Align displacement gage on the test beam over the notch using the holding yoke described in Reference 7. A sketch of this is shown in Fig. 3.7.
2. Set appropriate scale factors on Plotter for load (Y-axis) and displacement (X-axis). A summary of X and Y axis scale settings follows:

Plotter: 431.13A - 02 (Type 200 Control Module)

X-axis METRIC SETTING

Ranges using calib. setting:

0.5% per cm = 0.05 V/cm
1.0% per cm = 0.10 V/cm
2.5% per cm = 0.25 V/cm
5.0% per cm = 0.50 V/cm
10.0% per cm = 1.0 V/cm

Using CMOD (Displacement) gage

Range 4: $\pm 2 \times 10^{-3}$ in./10V = $\pm 2 \times 10^{-4}$ in./V

0.5% : 1 cm = 1×10^{-5} in.
1.0% : 1 cm = 2×10^{-5} in.
2.5% : 1 cm = 5×10^{-5} in.
5.0% : 1 cm = 1×10^{-4} in.

Range 3: $\pm$ 4 x 10^{-3} in./10V = $\pm$ 4 x 10^{-4} in./V

0.5% : 1 cm = 2 x 10^{-5} in.

1.0% : 1 cm = 4 x 10^{-5} in.

2.5% : 1 cm = 1 x 10^{-4} in.

5.0% : 1 cm = 2 x 10^{-4} in.

Range 2: $\pm$ 1 x 10^{-2} in./10V = $\pm$ 1 x 10^{-3} in./V

0.5% : 1 cm = 5 x 10^{-5} in.

1.0% : 1 cm = 1 x 10^{-4} in.

2.5% : 1 cm = 2.5 x 10^{-4} in.

5.0% : 1 cm = 5 x 10^{-4} in.

Range 1: $\pm$ 2 x 10^{-2} in./10V = $\pm$ 2 x 10^{-3} in./V

0.5% : 1 cm = 1 x 10^{-4} in.

1.0% : 1 cm = 2 x 10^{-4} in.

2.5% : 1 cm = 5 x 10^{-4} in.

5.0% : 1 cm = 1 x 10^{-3} in.

Y-axis METRIC SETTING

Ranges using calib. setting the same as X-axis.

Using load cell with X 10

1V = 1000 lb.

0.5% : 1 cm = 50 lb.

1.0% : 1 cm = 100 lb.

2.5% : 1 cm = 250 lb.

5.0% : 1 cm = 500 lb.

3. Operate system in load control.
4. Use ramp function and span (frequency = 0.05)
5. Apply 0.60 Pmax using span control to obtain load V CMOD curve, then measure straight slope and determine compliance.
6. Reload to failure and trace entire load V CMOD curve. This process can be done very quickly.

Static crack growth of specimens without teflon

Steps 1 through 4 listed previously in Section 3.3 are the same here, except in step 3, that the system operated in strain (CMOD) control.

5. Apply load using span control. As cracking starts the slope of the load-displacement plot decreases. At this point the load is removed.
6. Measure the straight slope of the curve and determine the crack length using the compliance calibration curves (Figs. 4.1-4.6). In fact, what was actually done, was to directly compare slopes of P-CMOD curves with those from the calibration beams for a particular notch depth.
7. Repeat steps 5 and 6 until the desired crack length is obtained. This process can be done fairly quickly and easily after the operator has gained some experience with the equipment. The entire process of statically cracking a beam to a desired crack length can be done in an hour or less and involves perhaps ten to twenty iterations of steps 5 and 6. However, difficulties in stability of the equipment are encountered for long cracks ($\frac{a}{w} > 0.6$).

A typical trace from the plotter showing this process is given in Fig. 3.3.

Load to failure

After all specimens were precracked they were immediately loaded to failure. This was done using load control and the ramp function. Typically the load was applied at a rate of 0.1-V per 10 seconds. This corresponds to about 10 lb. per second (44.5 N per second) and a CMOD rate of about 1.0×10^{-4} in./sec. (2.54×10^{-3} mm./sec.) initially. The failure load was taken as the peak load recorded.

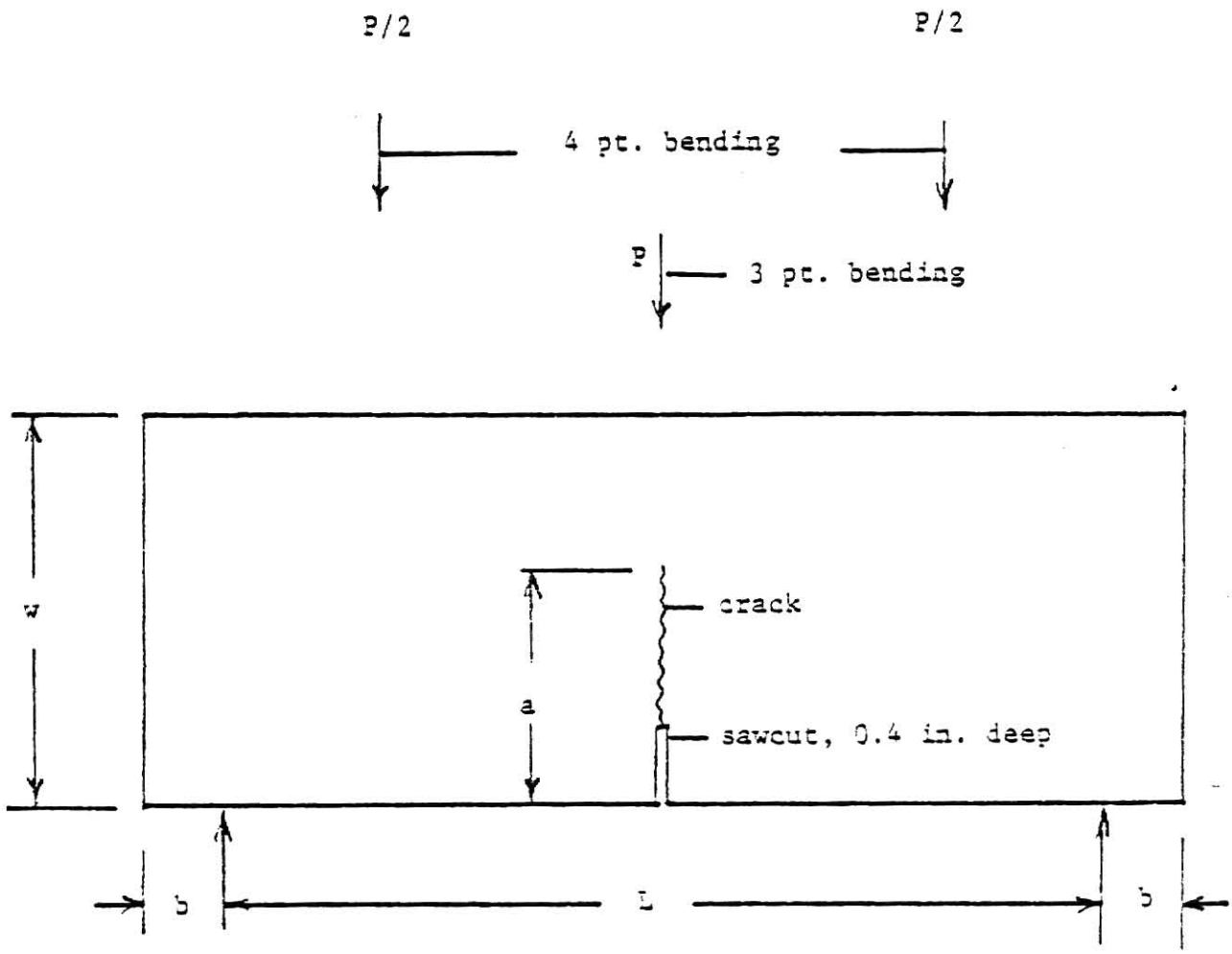

Specimen width = C = 3 in.

Fig. 3.1 Test Specimen and Loading Geometry,
1 in. = 25.4 mm

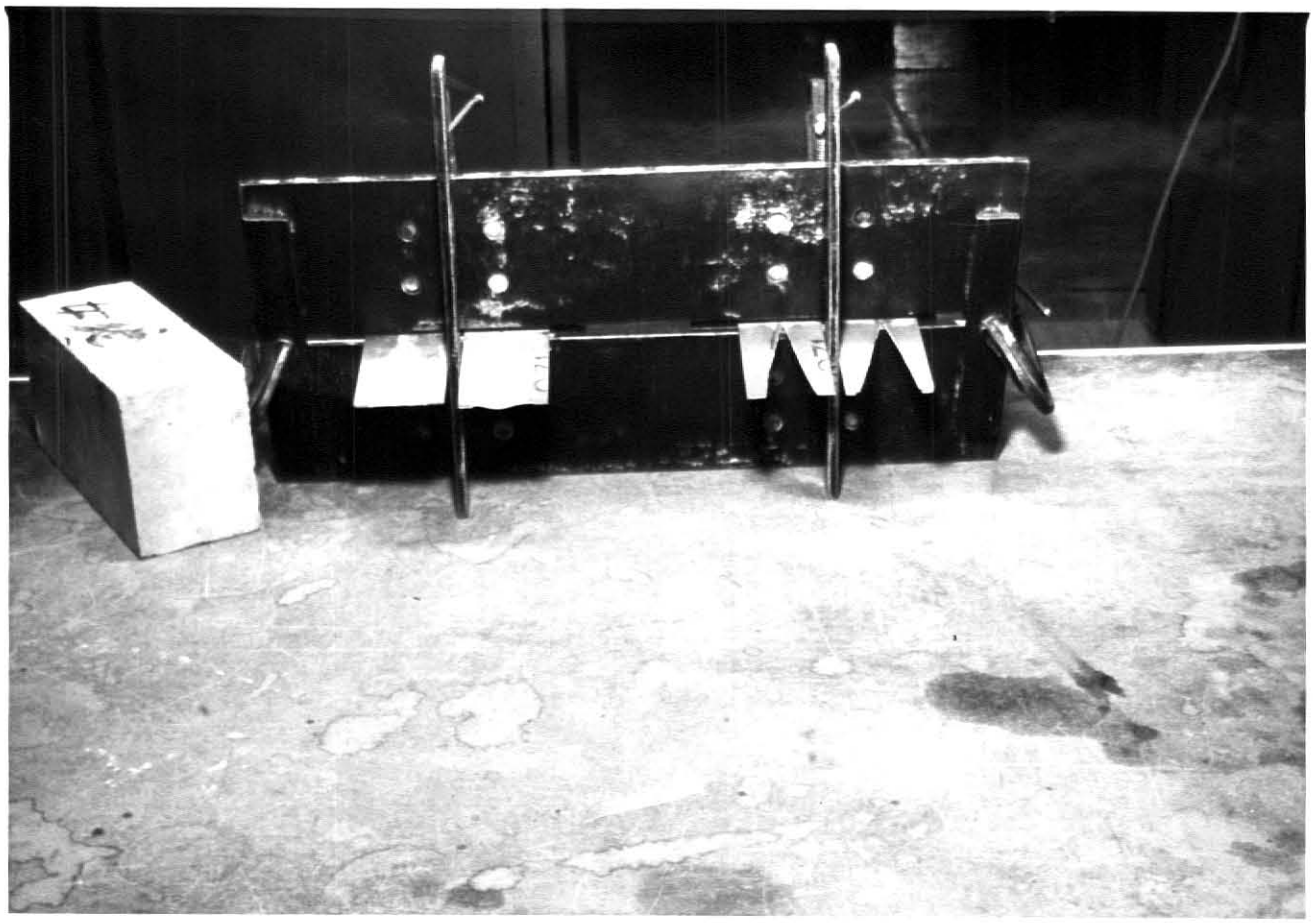

Fig. 3.2 - Holders for Teflon Inserts

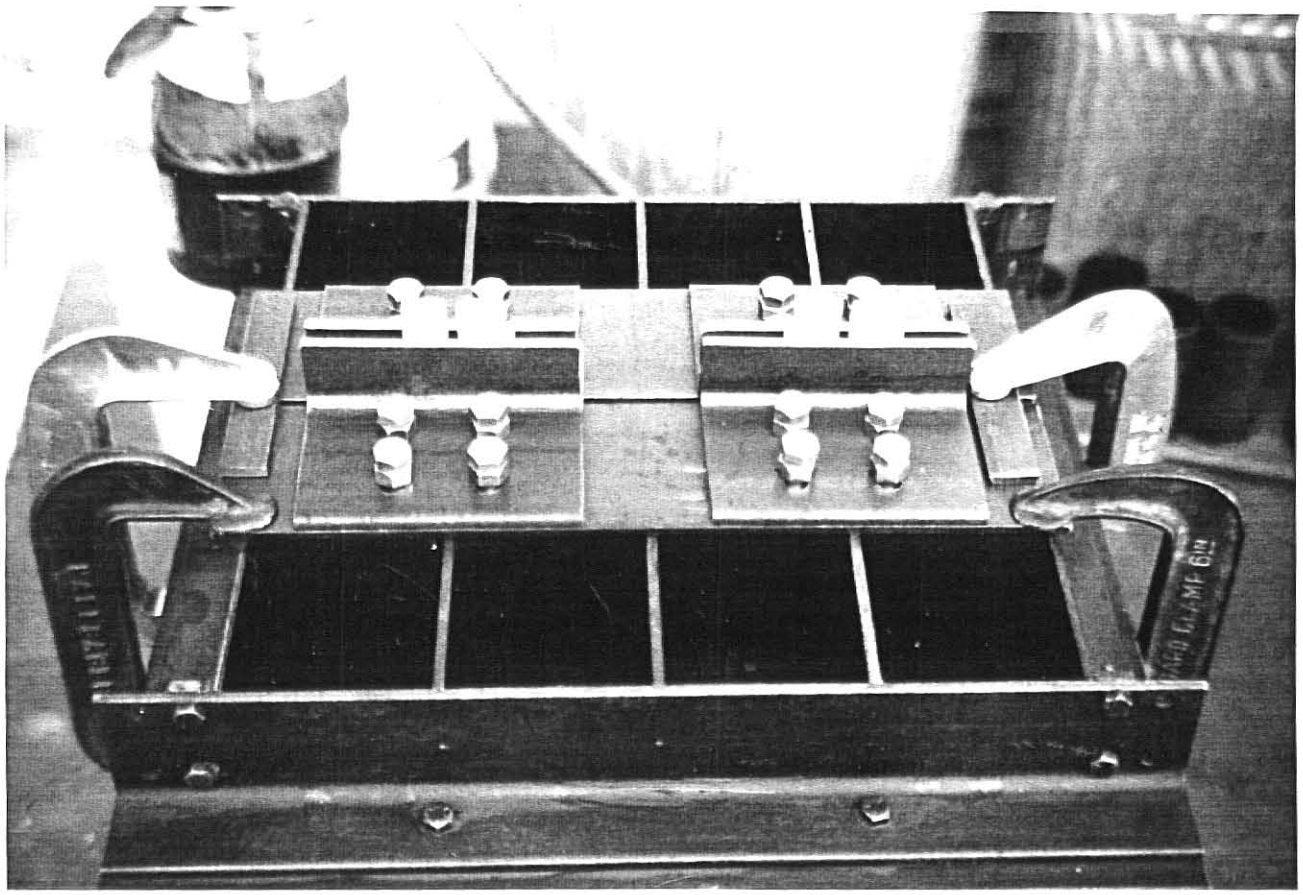

Fig. 3.3 - Beams Mold Modified for Teflon Inserts

Fig. 3.4 - Beams Removed from Molds

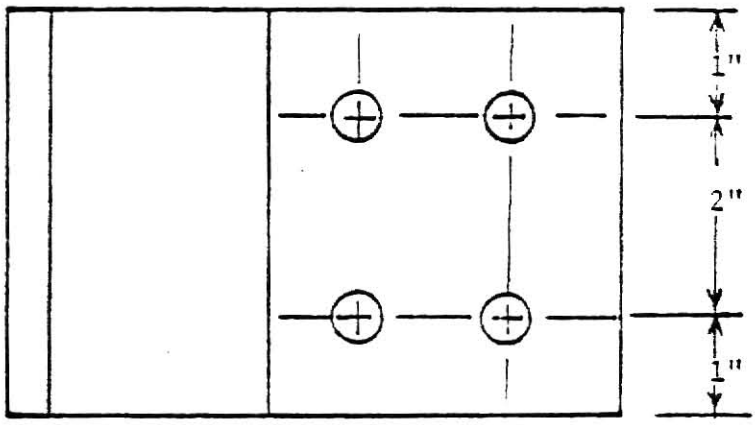

Plan

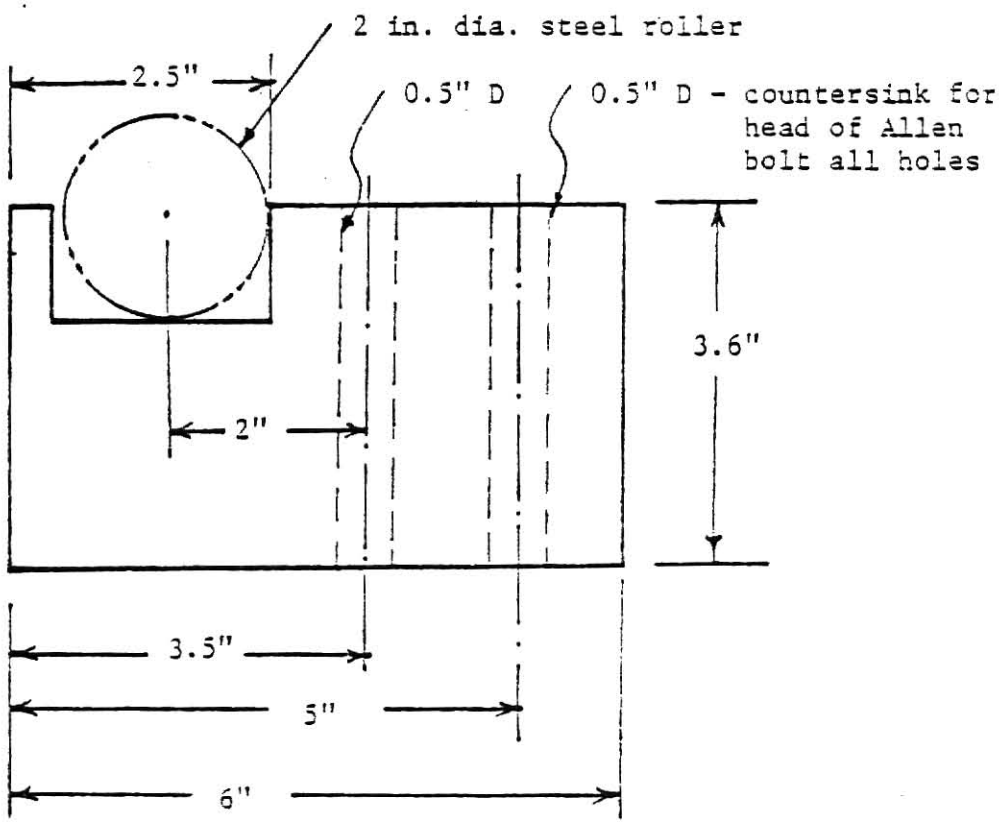

Elevation

Fig. 3.5 Roller Support Blocks,
1 in. = 25.4 mm.

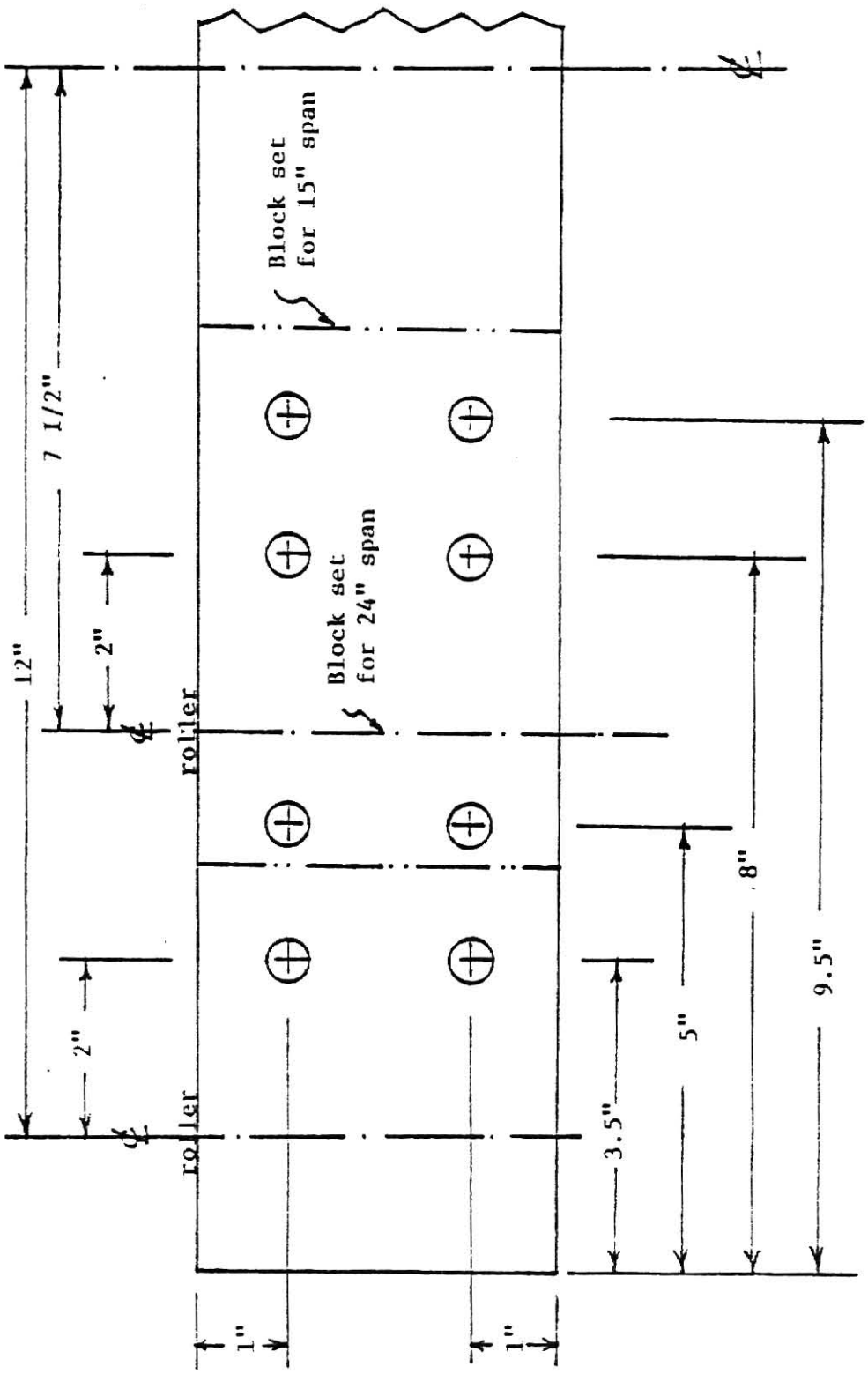

Plat thickness, 0.5 in.

All holes, 0.5" D, tapped for 1/2 in.

Allen head bolt

Fig. 3.6 Support Plate for Roller Support Blocks,
1 in. = 25.4 mm.

ILLEGIBLE DOCUMENT

THE FOLLOWING DOCUMENT(S) IS OF POOR LEGIBILITY IN THE ORIGINAL

THIS IS THE BEST COPY AVAILABLE

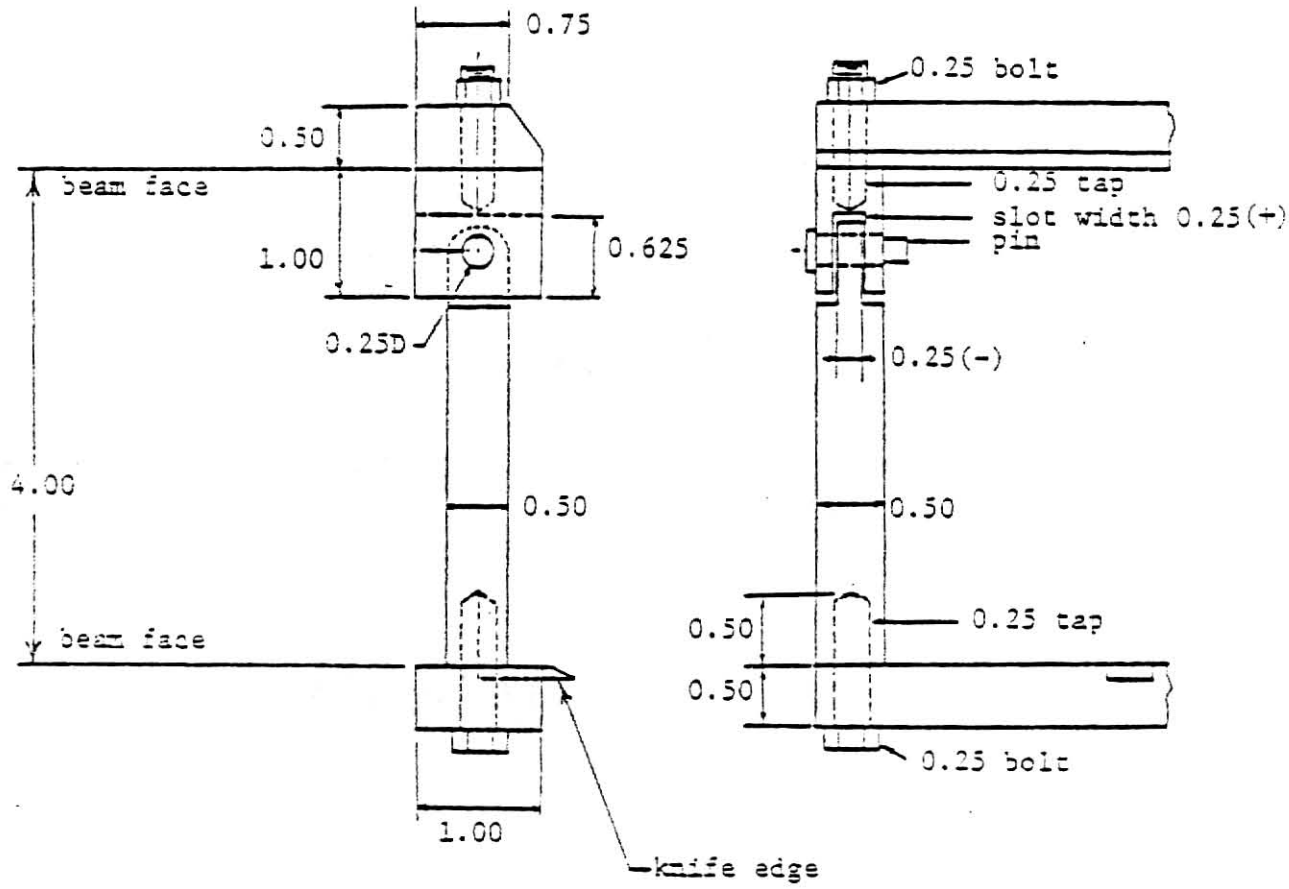

Elevation End

All dimensions inches

Fig. 3.7 Displacement Gage Yoke,
1 in. = 25.4 mm.

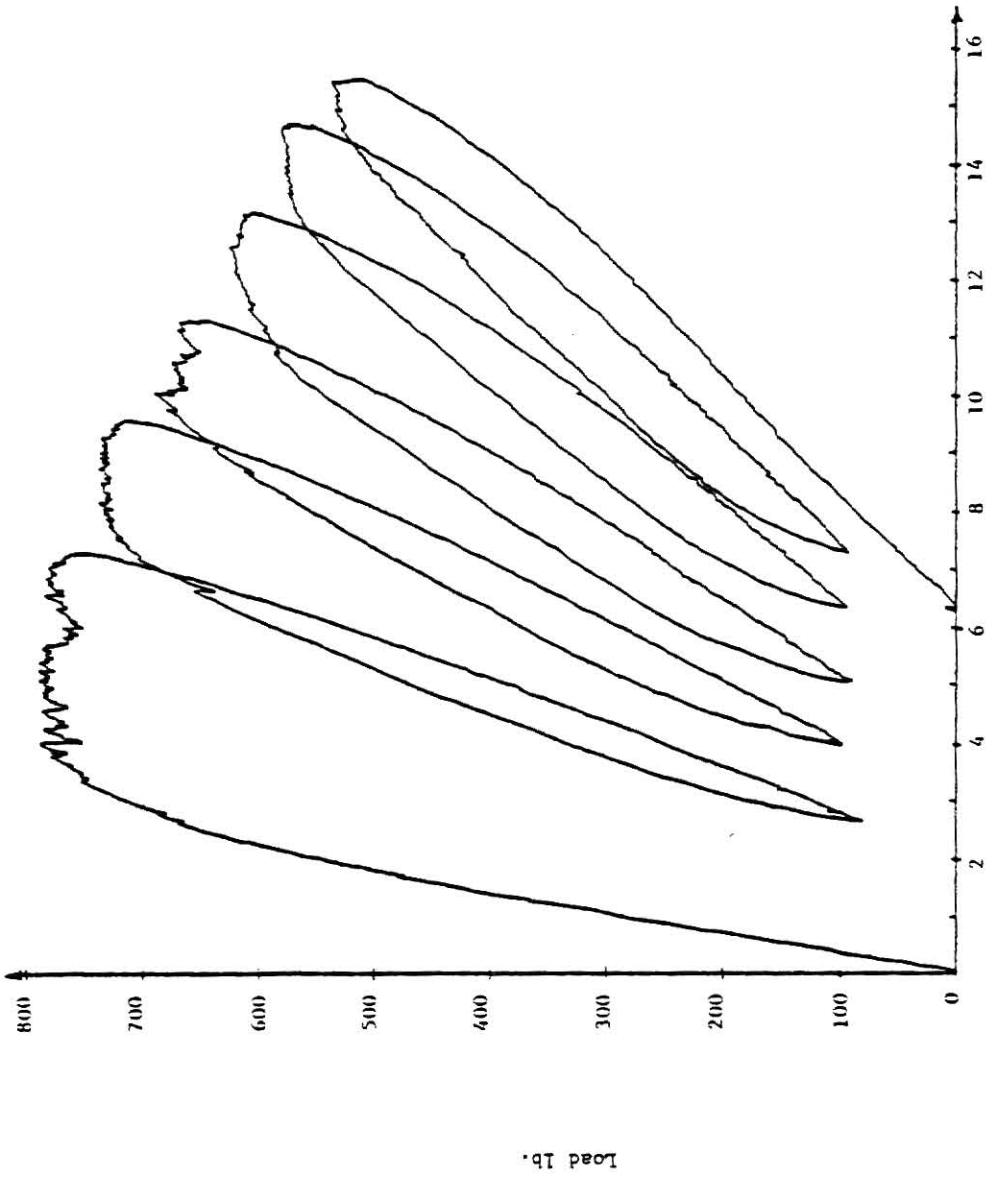

Fig. 1.8 - Trace of P V CMOD for Static Crack Growth (2-A.11), 1 lb. = 4.45 N, 1 in. = 25.4 mm.

Chapter 4

TEST RESULTS

A total of 96 beams were constructed. Twelve of these beams were used for compliance calibration specimens and the remainder were tested as described previously. The data that were collected, are presented separately for each batch for each mix in tabular form at the end of this chapter. (Tables 4.1-4.12). The theoretical relationship between K_I and a/w which has been used to evaluate the data obtained from this experiment was obtained from a finite-element computer program developed by Hu and Huang.* From this computer program two curves have been drawn, Figs.4.7,4.8, (K_I $\underline{V}$ a/w) for a unit load for three and four-point bending for the beam geometry used here.

A total number of 30 cylinders, (3 in. x 6 in.), were made. Batch 1-A had three cylinders and all were tested in compression without strain gages. Batch 2-A had five cylinders, four were tested with the compression machine and one with the tension machine (no strain gages were used in this batch). Batch 3-A had six cylinders, five for compression testing (four tested without strain gages and one with strain gages), one for tension testing using strain gages. Batch 1-B had six cylinders, five for compression and one for tension testing (no strain gages were used in this batch). Batch 2-B had five cylinders, four for compression testing without strain gages and one for compression testing with strain gages. Batch 3-B had five cylinders, all were used for compression testing without strain gages.

The mix A nominal strength was 3200 psi (22.07 MPa) and mix B nominal strength was 6700 psi (46.21 MPa).

* Civil Engineering Dept., Kansas State University; under development - not generally available at this time.

Two beams of each batch were used for compliance calibration. Recording $\frac{a}{w}$ and computing compliance by using the inverse slope for each value of a/w, a compliance calibration curve was drawn (compliance V a/w) Figs. 4.1-4.6. The net bending stress for each beam was calculated from the data obtained during the experiment. The average bending stress and average a/w for each batch were obtained then plotted in Figs. 4.9, 4.10. These results definitely indicate both mixes yielded notch-sensitive specimens.

All values of stress intensity were plotted versus a/w for mix A in Fig. 4.11 and for mix B in Fig. 4.12. Using a least squares computer program, a second order polynomial curve was plotted through each set.

Average stress intensity values are plotted versus average a/w in Fig. 4.13 (a) and (b) for mix A and mix B respectively. It can be seen from these figures that by increasing a/w, the values of stress intensity decrease.

Computing the ratios of stress intensity values for precracked beams divided by the stress intensity values for prenotched beams and using the average values of a/w for mixes A and B, six points were plotted. Using these six points, an equation has been derived as a function of a/w and does not depend on other variables. This equation is

$$\frac{K_{IP}}{K_{IT}} = 0.9137 + 1.6118 \left(\frac{a}{w}\right).$$

For simplicity this equation is modified to be

$$K_{IP} = \left(1.0 + 1.6 \frac{a}{w}\right) K_{IT} \quad . \quad . \quad . \quad . \quad (1)$$

where K_{IP} = stress intensity value for precracked beams,

K_{IT} = stress intensity value for prenotched beams (with teflon),

a = crack depth,

w = depth of beam

Both of these equations are plotted in Fig. 4.14.

Two beams (2-A.11 and 3-A.14) out of the forty-two beams that were tested by statically precracking were chosen to obtain K_I values using the approach of Hillemeir, et al. A trace of load cycles for beam 2-A.11 is shown in Fig. 3.8. Stress intensity values for each depth of crack were calculated and then plotted versus a/w. For the two beams selected these are shown in Figs. 4.15-4.16. Again as the crack depth increases, stress intensity decreases.

The failure surface appearance in the region beyond the initial crack for the beams with notches was identical to that for beams which were precracked as shown in Fig. 4.17.

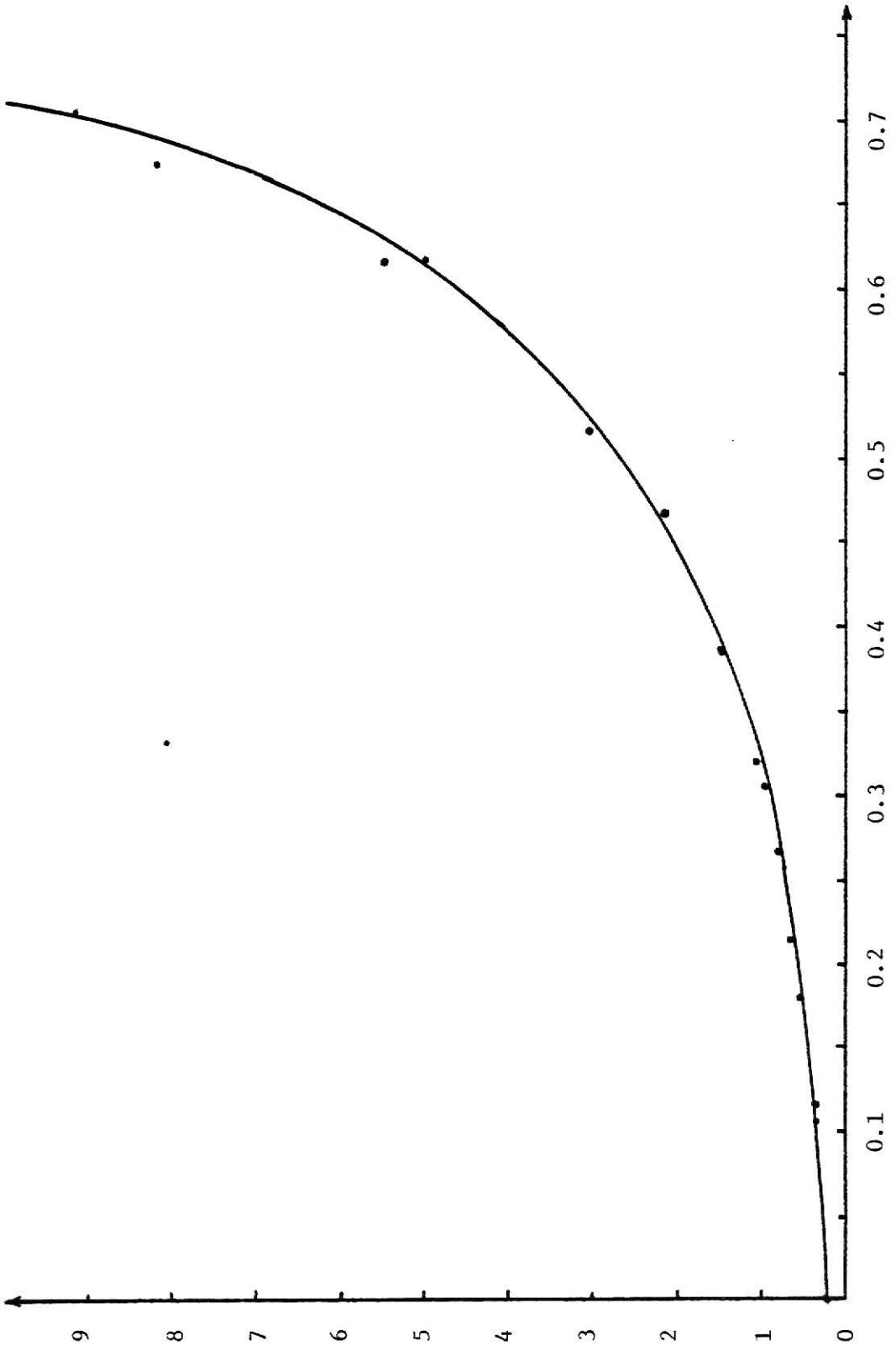

Fig. 4.1 - Compliance V Crack Depth/Beam Depth, Group 1-A

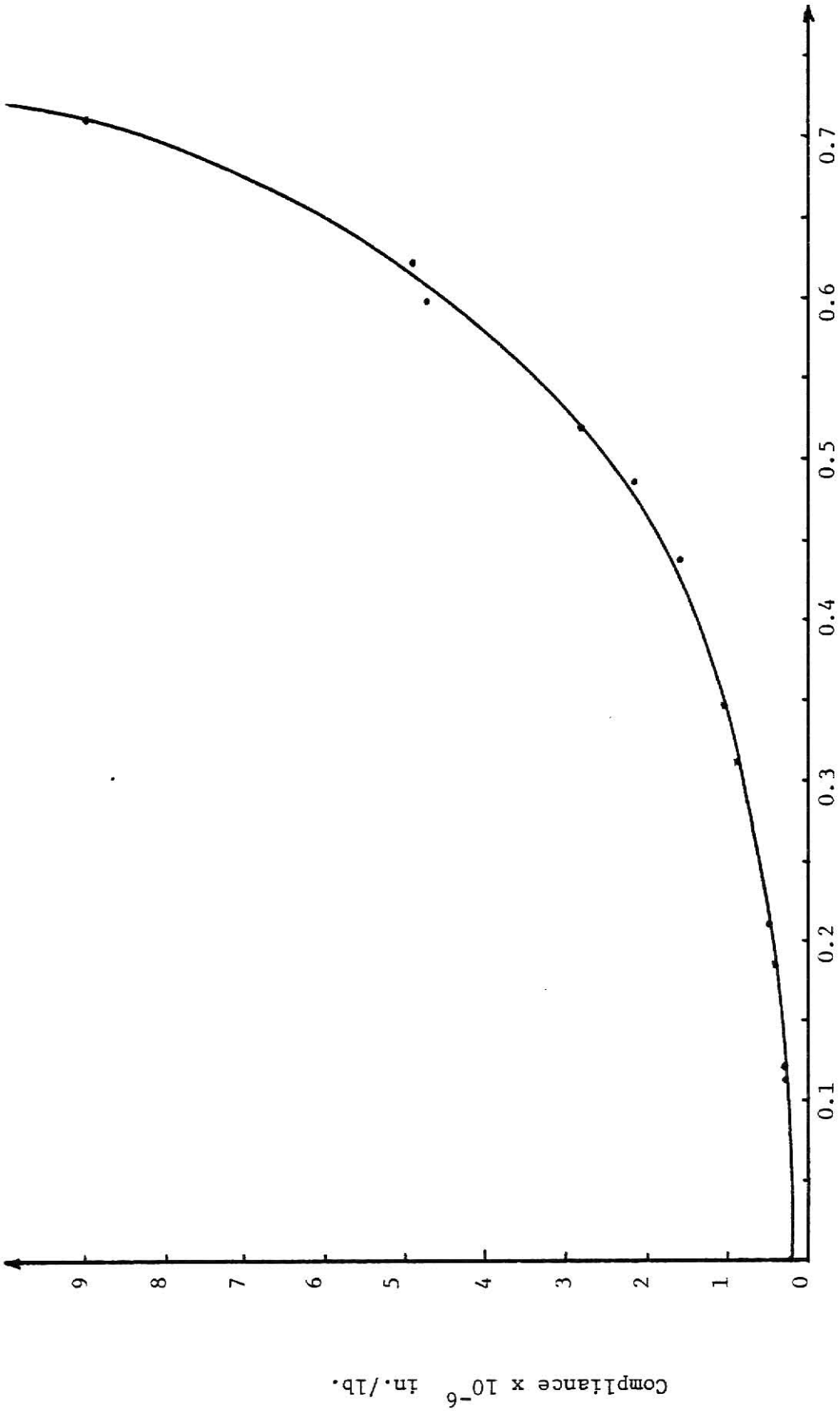

Fig. 4.2 - Compliance V Crack Depth/Beam Depth, Group 2-A

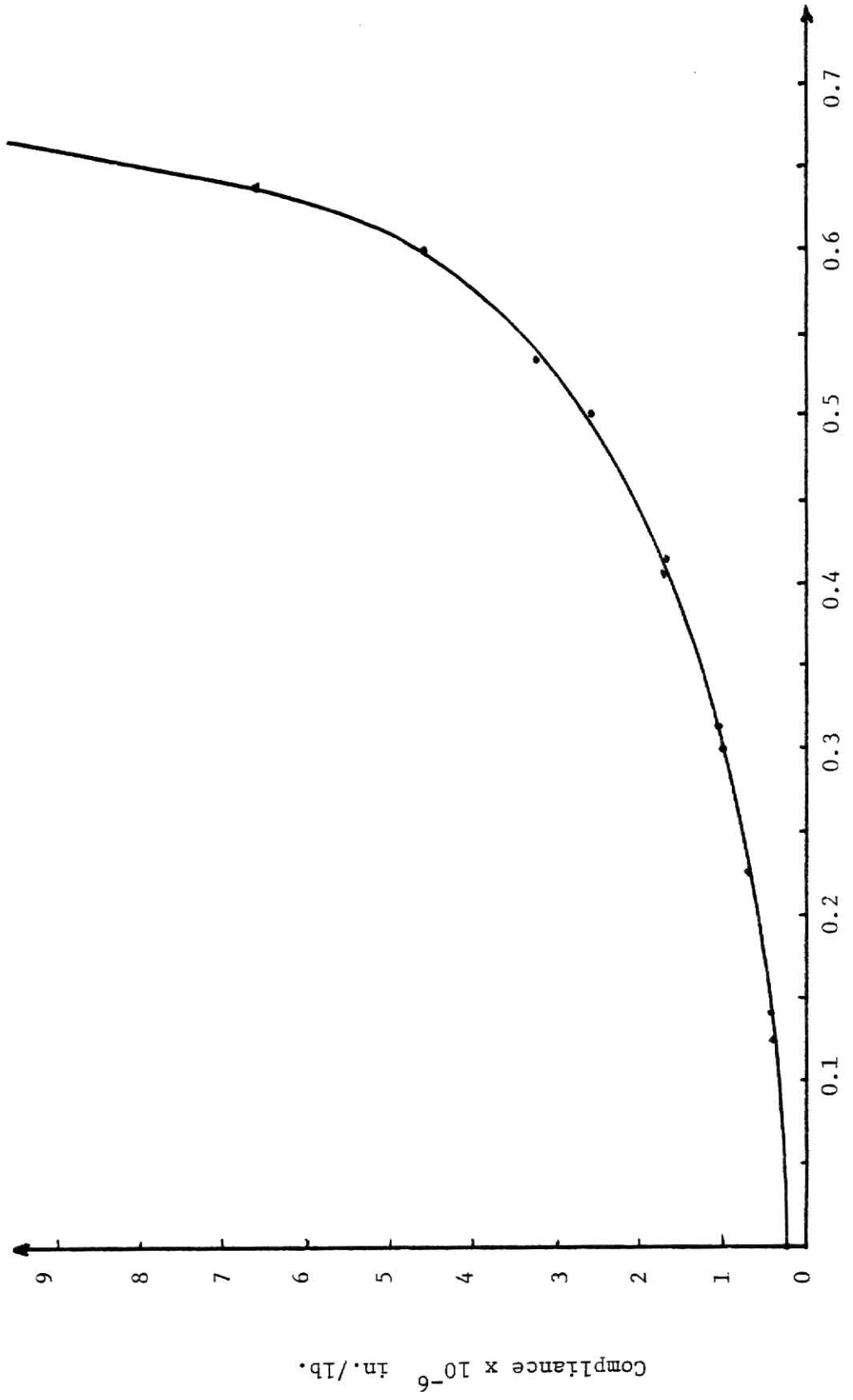

Fig. 4.3 - Compliance V Crack Depth/Beam Depth, Group 3-A

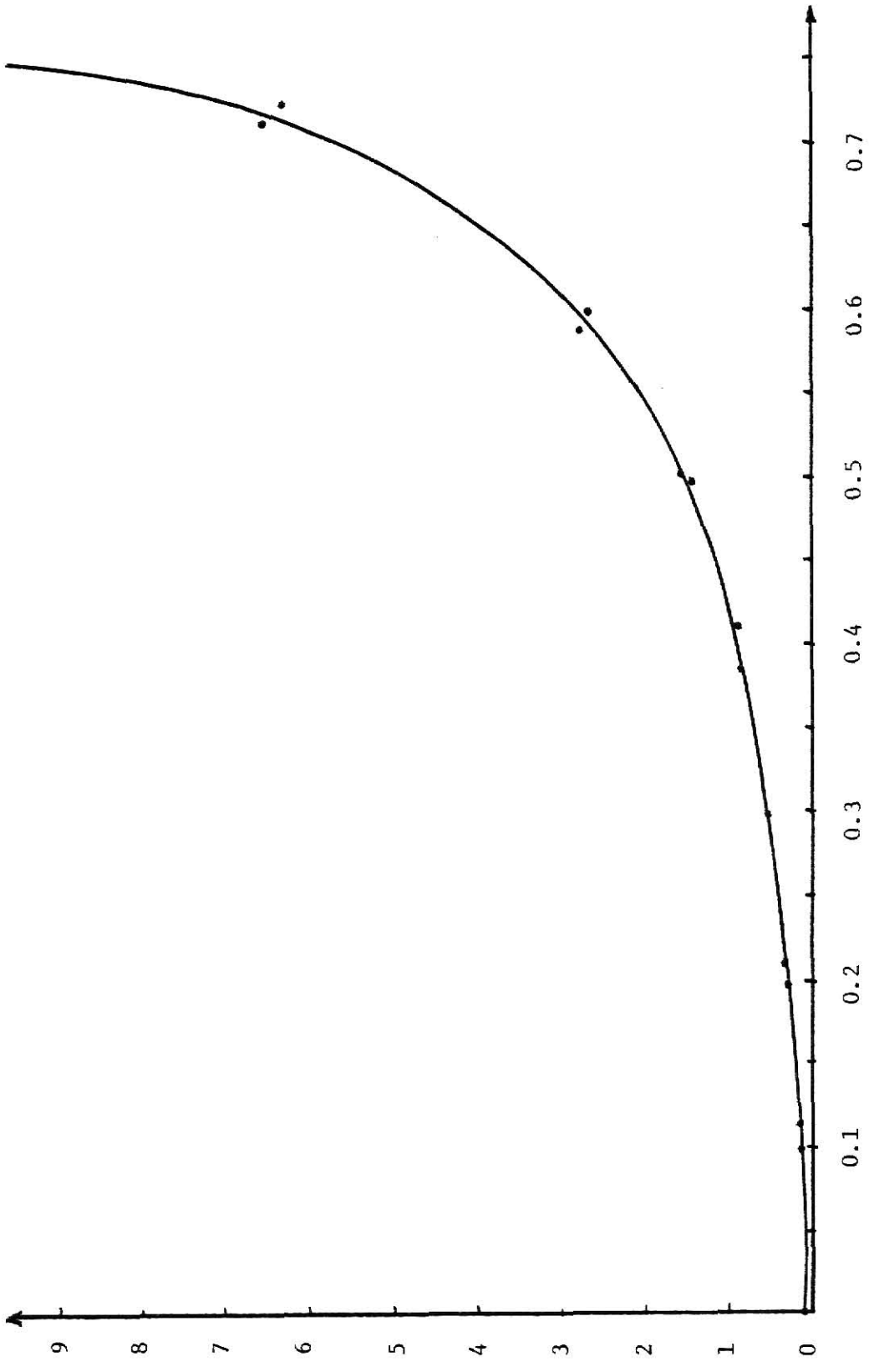

Fig. 4.4 - Compliance V Crack Depth/Beam Depth, Group 1-B

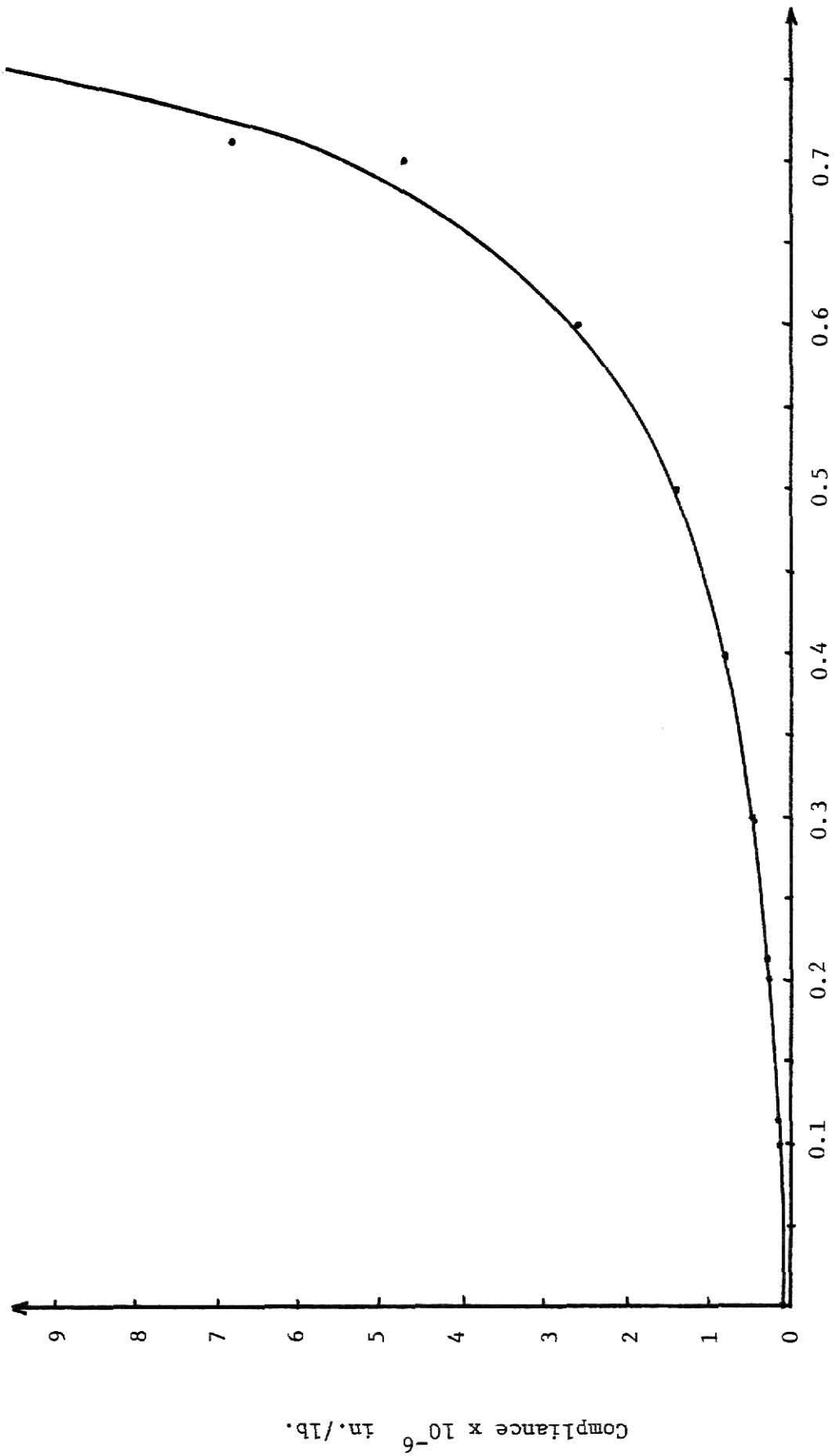

Fig. 4.5 - Compliance V Crack Depth/Beam Depth, Group 2-B

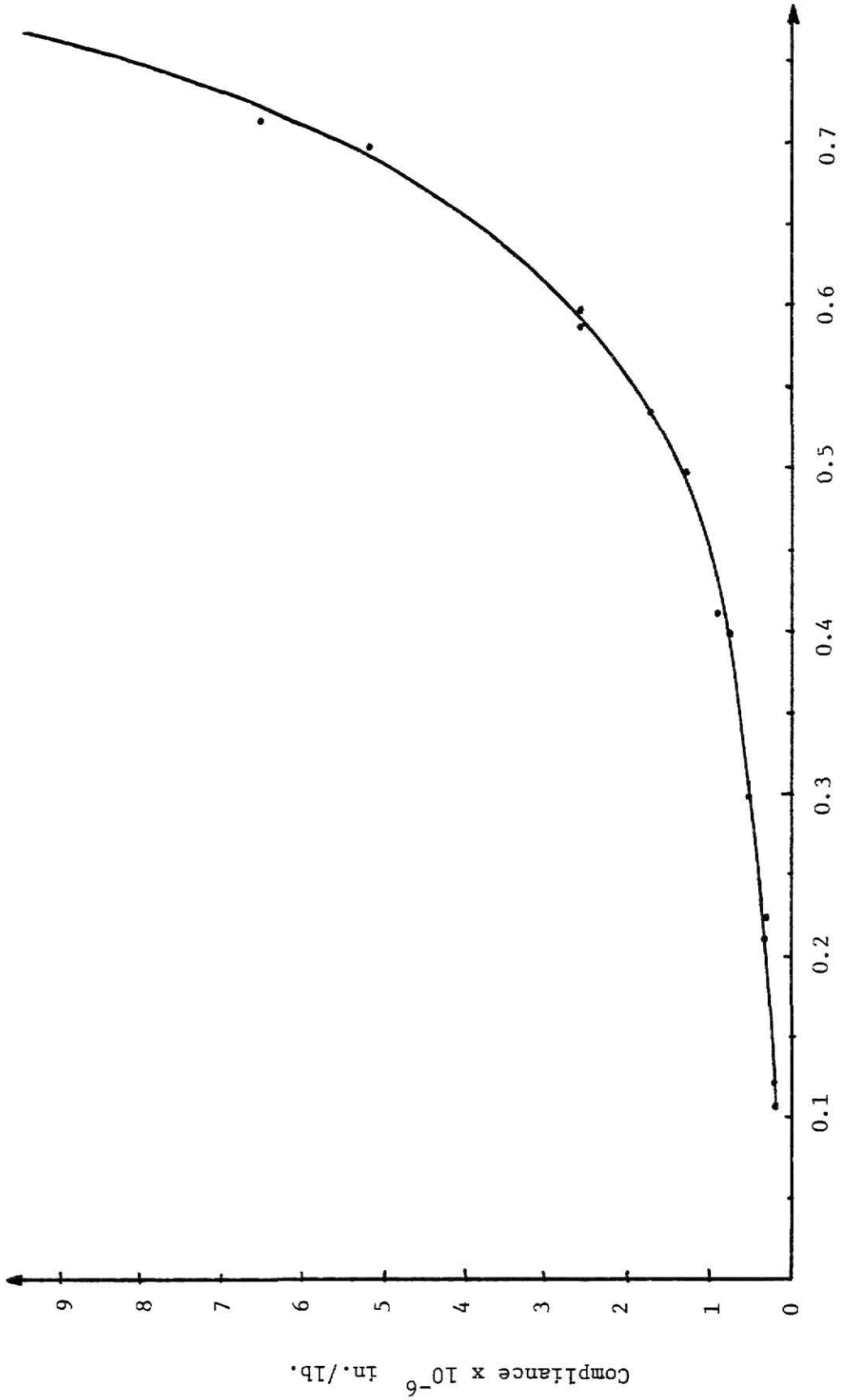

Fig. 4.6 - Compliance V Crack Depth/Beam Depth, Group 3-B

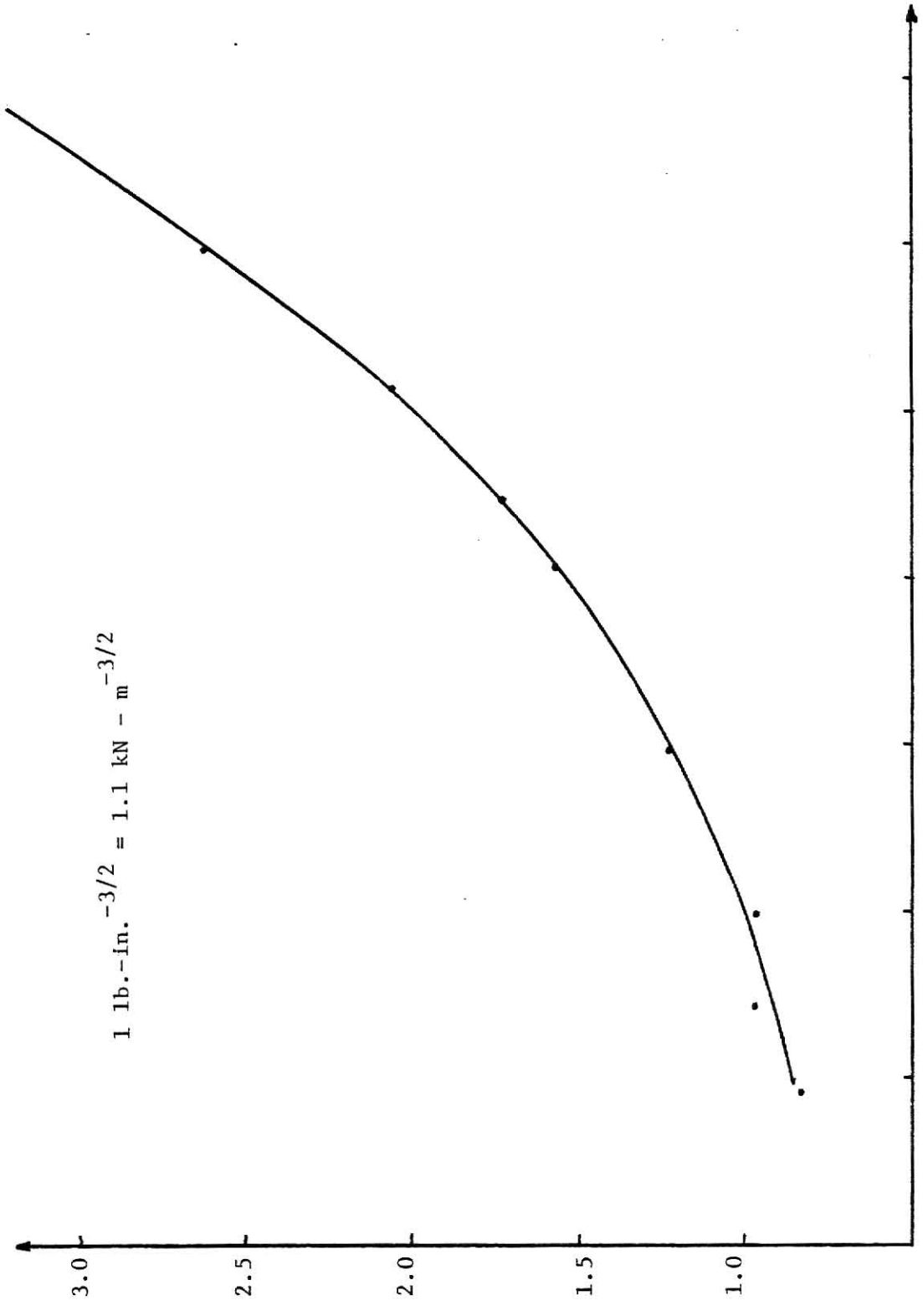

Fig. 4.7 - Stress Intensity (K_I) V Crack Depth/Beam Depth, Unit Load, 3 point bending

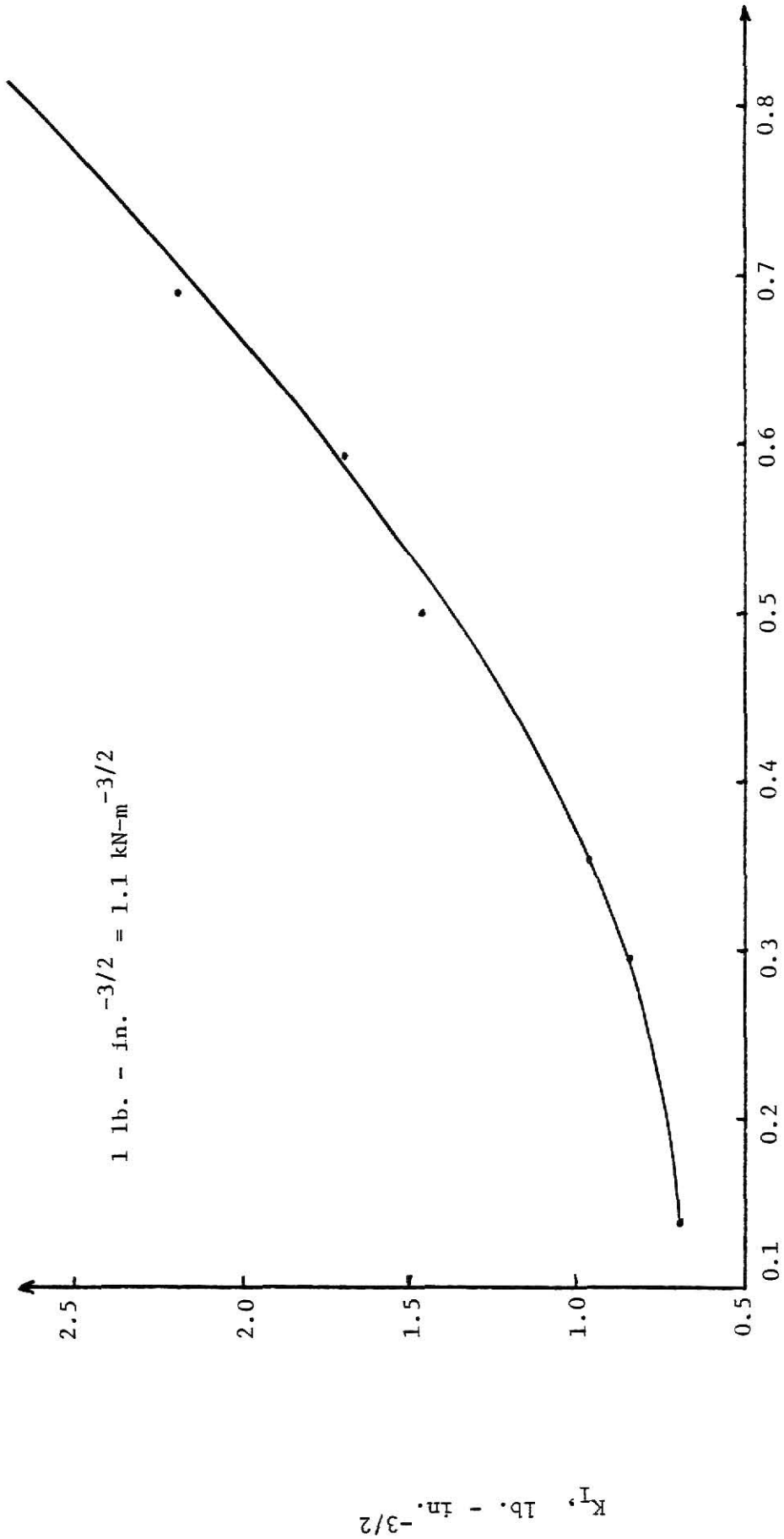

Fig. 4.8 - Stress Intensity (K_I) $\underline{V}$ Crack Depth/Beam Depth, Unit Load, 4 point bending

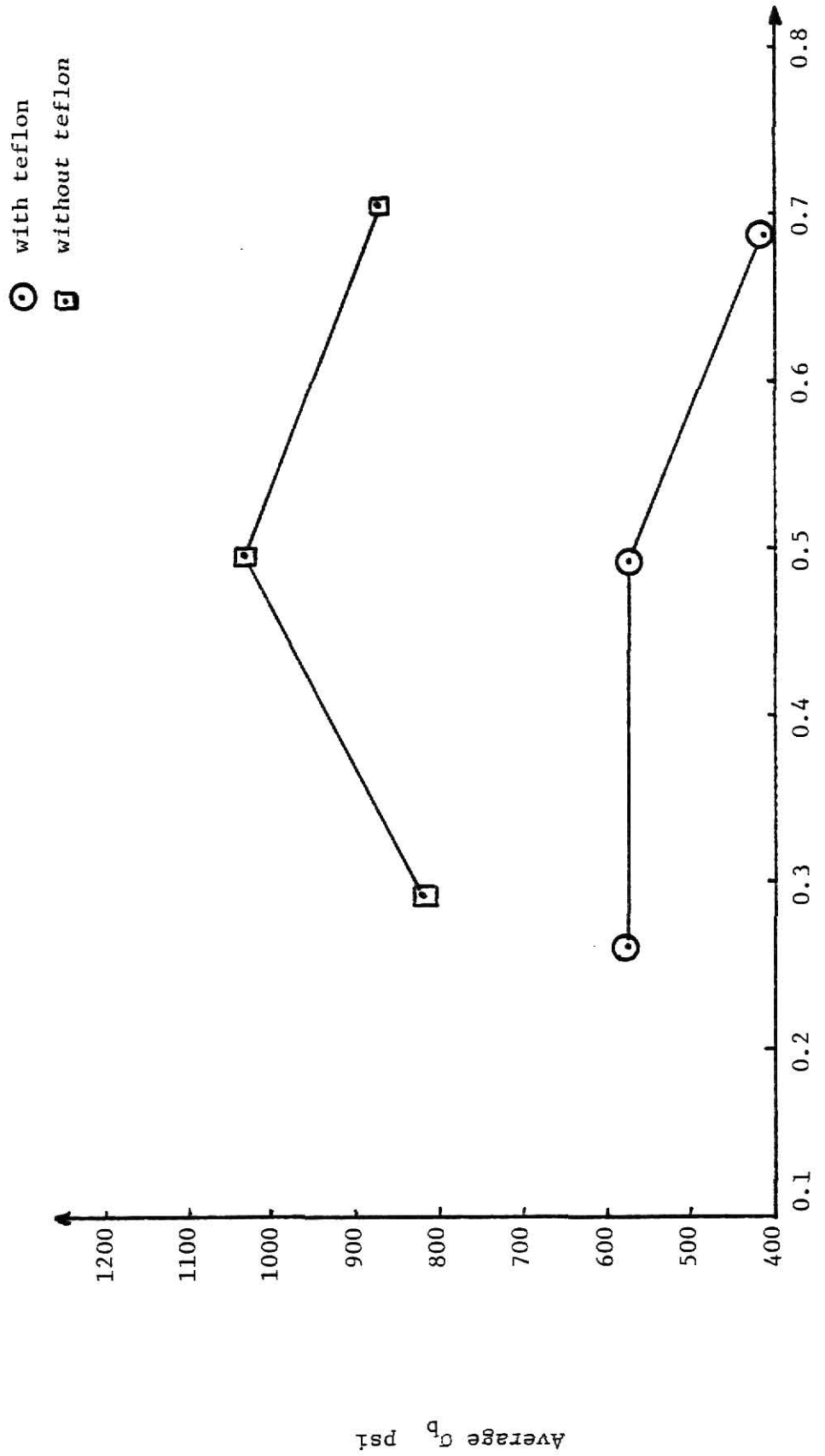

Fig. 4.9 - Average Bending Stress (σ_b), $\underline{V}$ Average Crack Depth/Beam Depth, Mix A
1 psi = 6.898 kPa

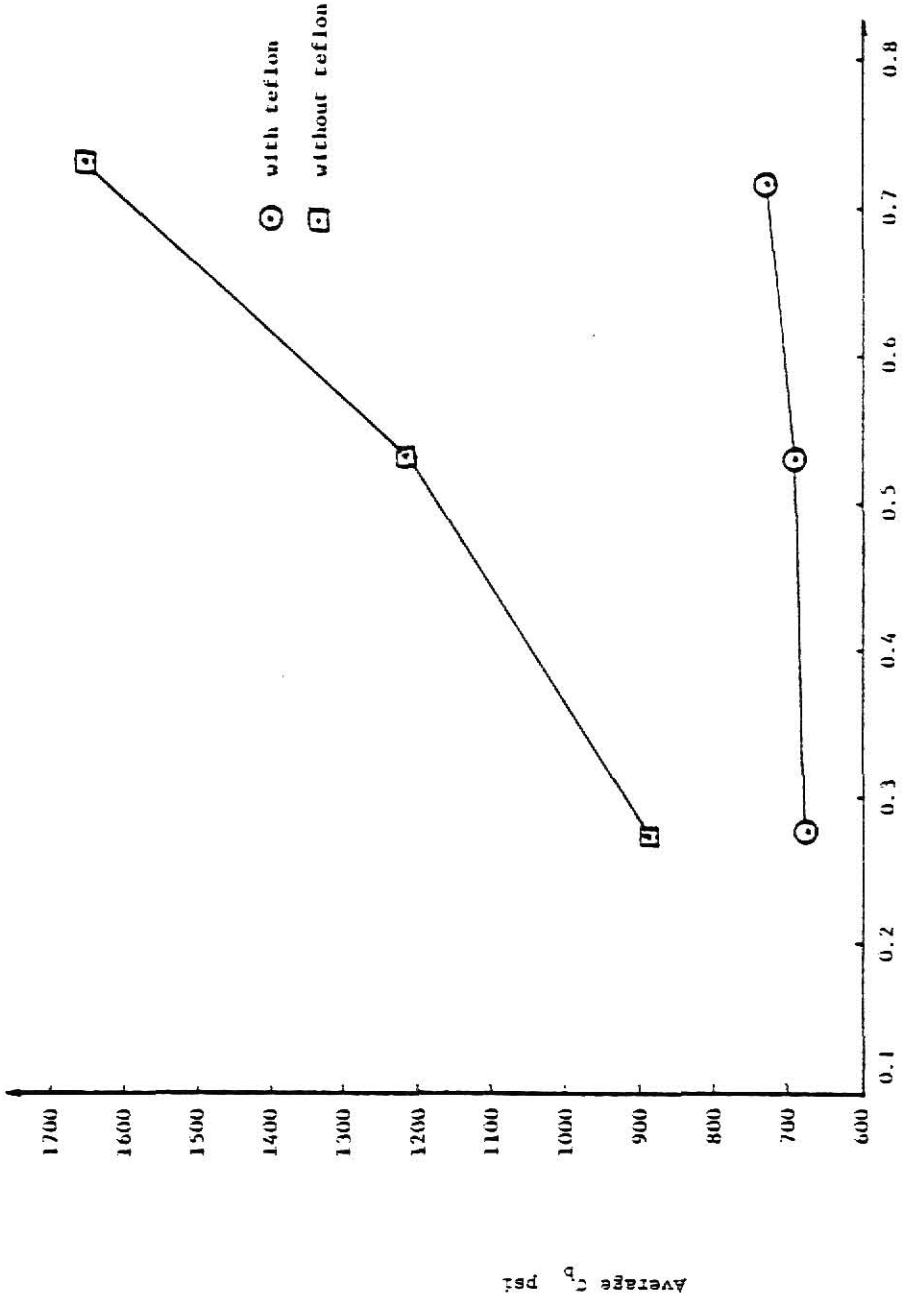

Fig. 4.10 - Average Bending Stress (σ_b) V Average Crack Depth/Beam Depth, Mix B
1 psi = 6.898 kPa

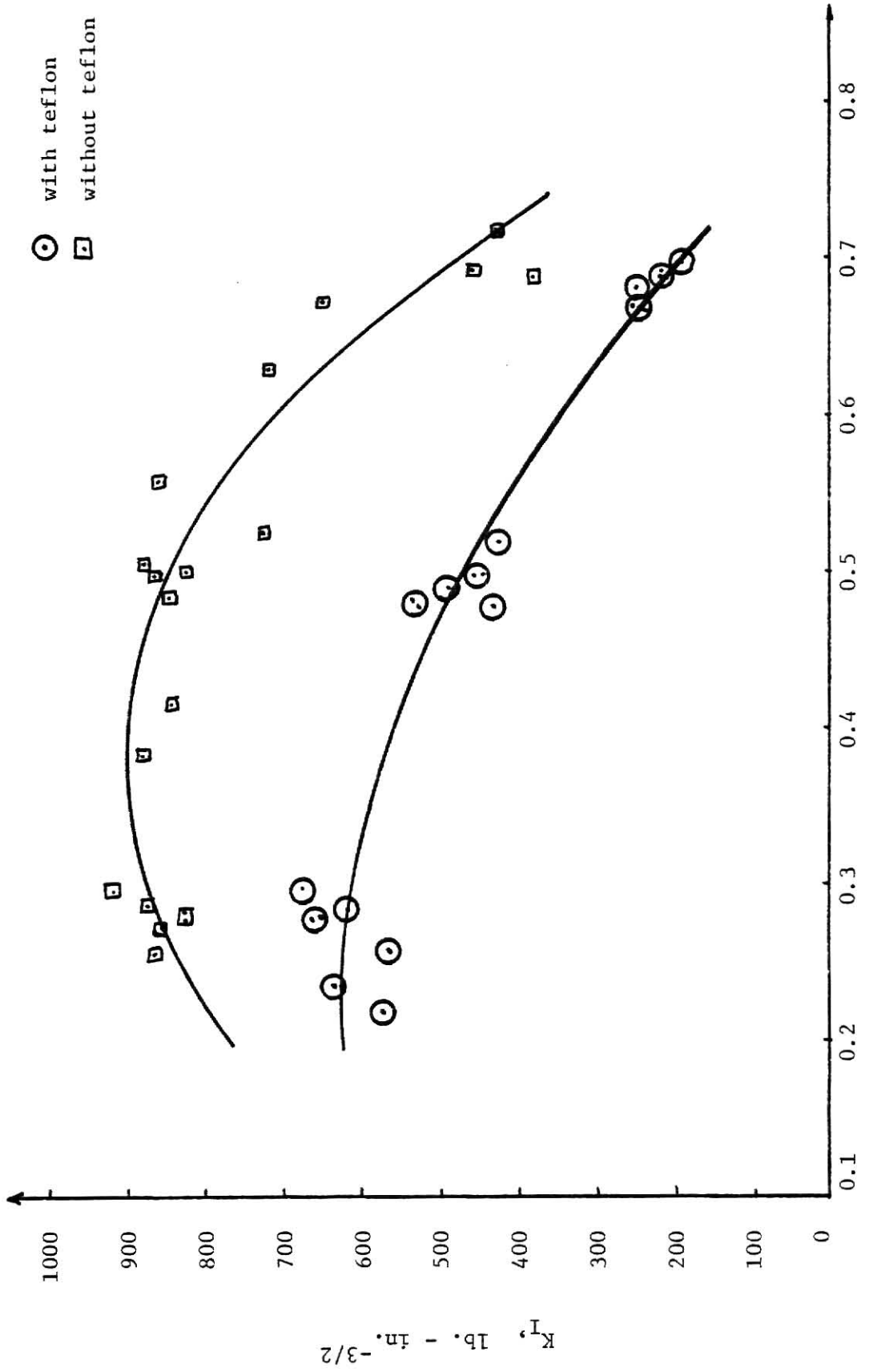

Fig. 4.11 - Stress Intensity (K_I) V Crack Depth/Beam Depth, Mix A

1 lb. - in.$^{-3/2}$ = 1.1 kN - m$^{-3/2}$

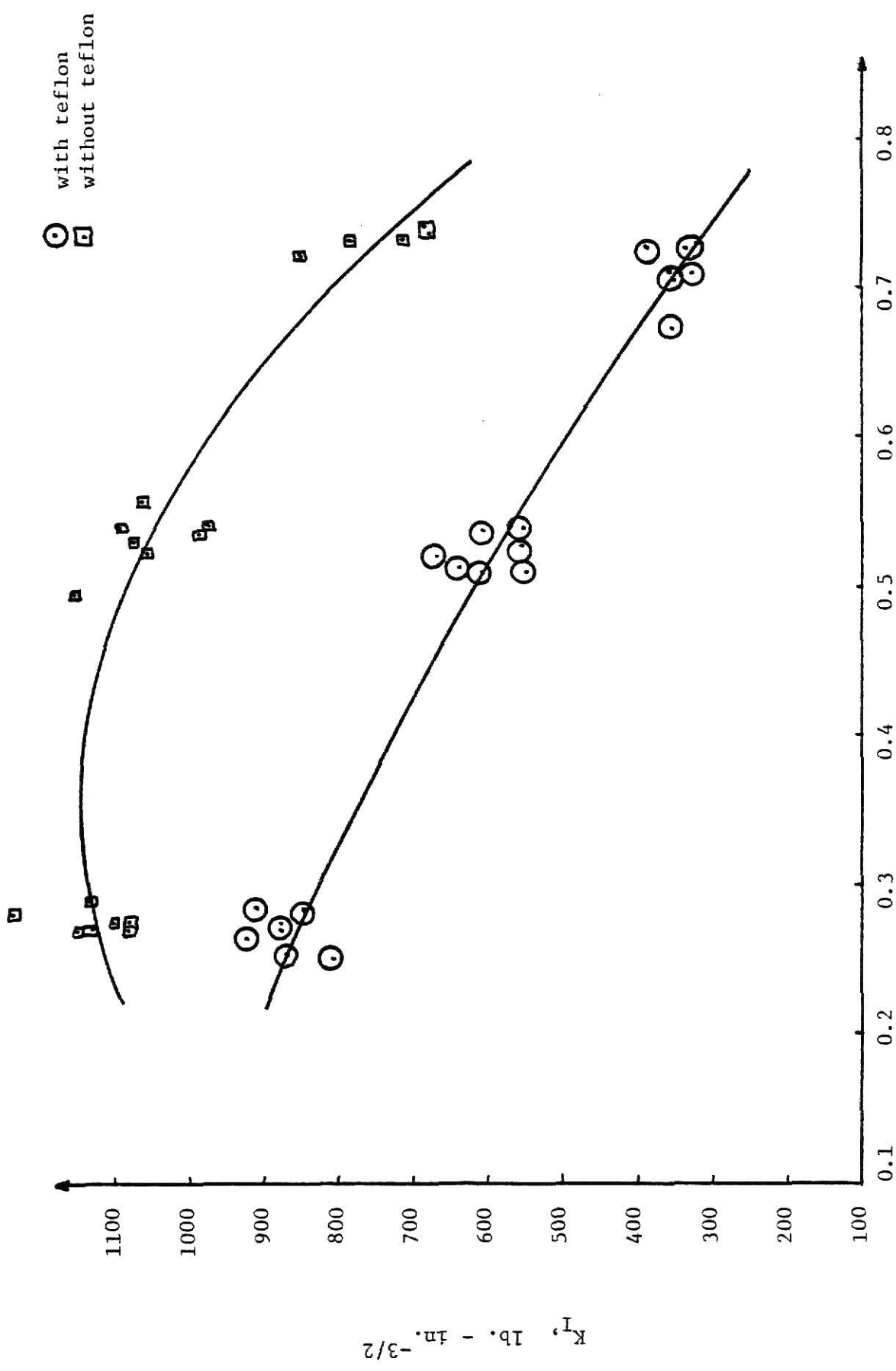

Fig. 4.12 - Stress Intensity (K_I) $\underline{V}$ Crack Depth/Beam Depth, Mix B,
$-3/2$ $-3/2$

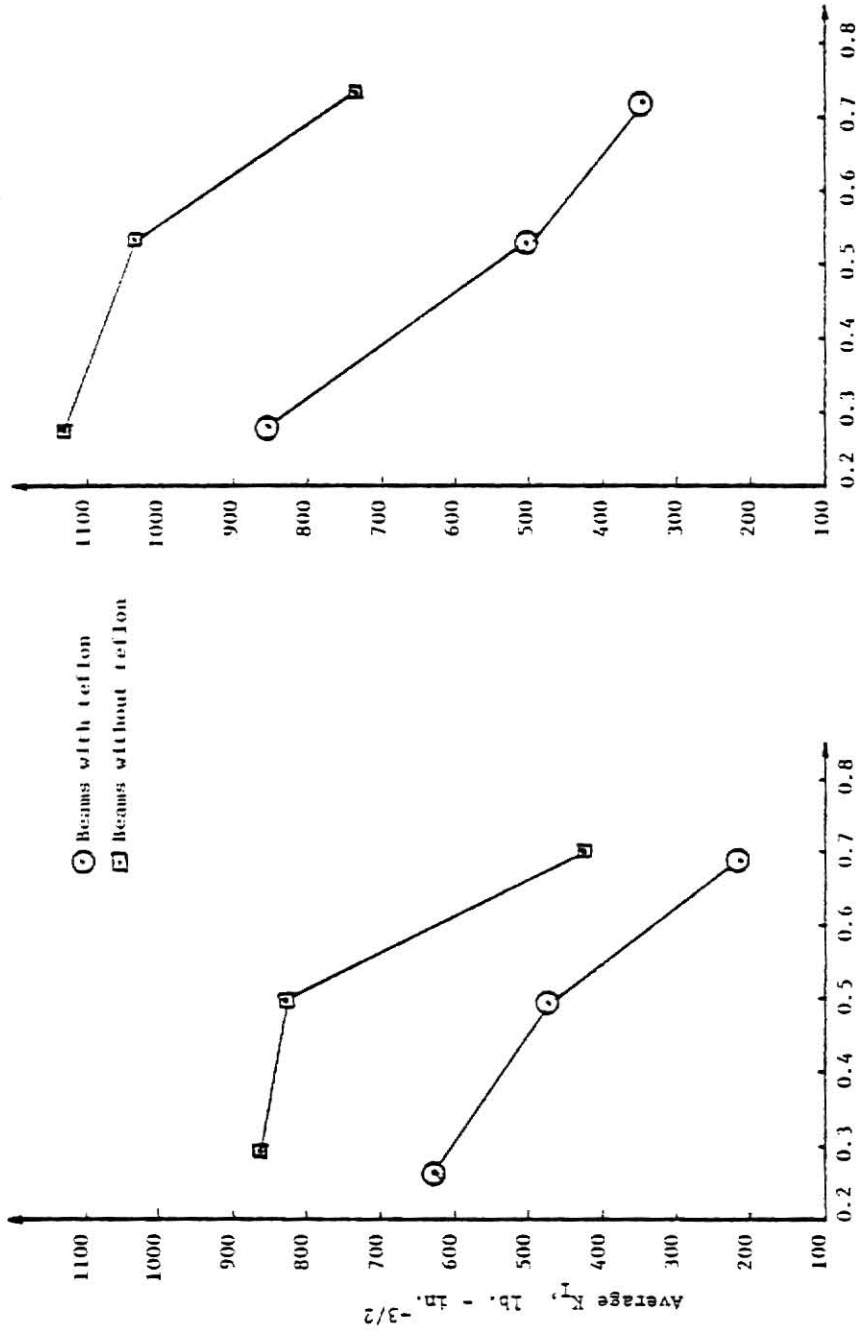

Fig. 4.13 - Average Stress Intensity (K_I) V Average Crack Depth/Beam Depth

1 lb. - in.$^{-3/2}$ = 1.1 kN - m$^{-3/2}$

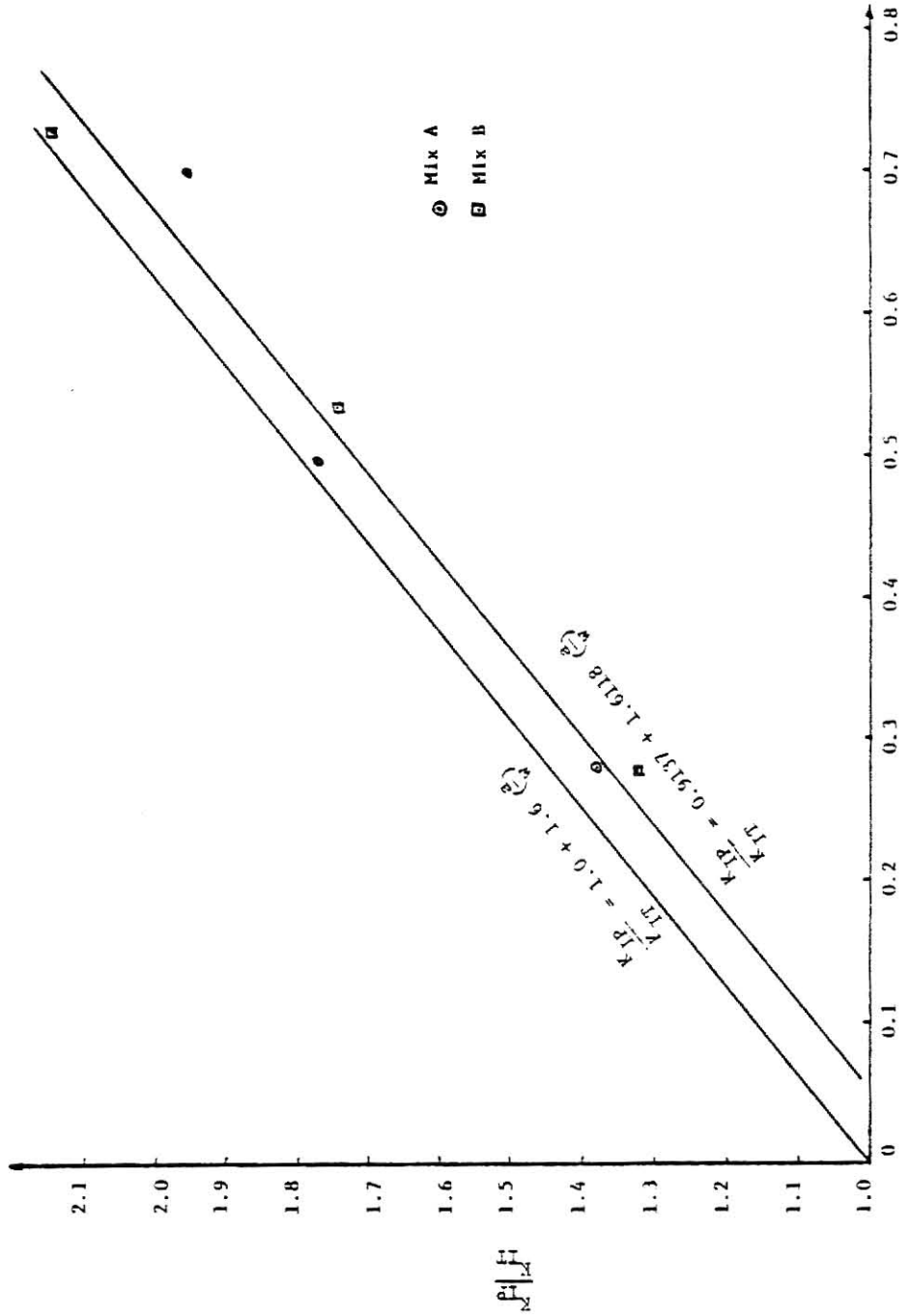

Fig. 4.14 - Stress Intensity Ratio Y Average Crack Depth/Beam Depth

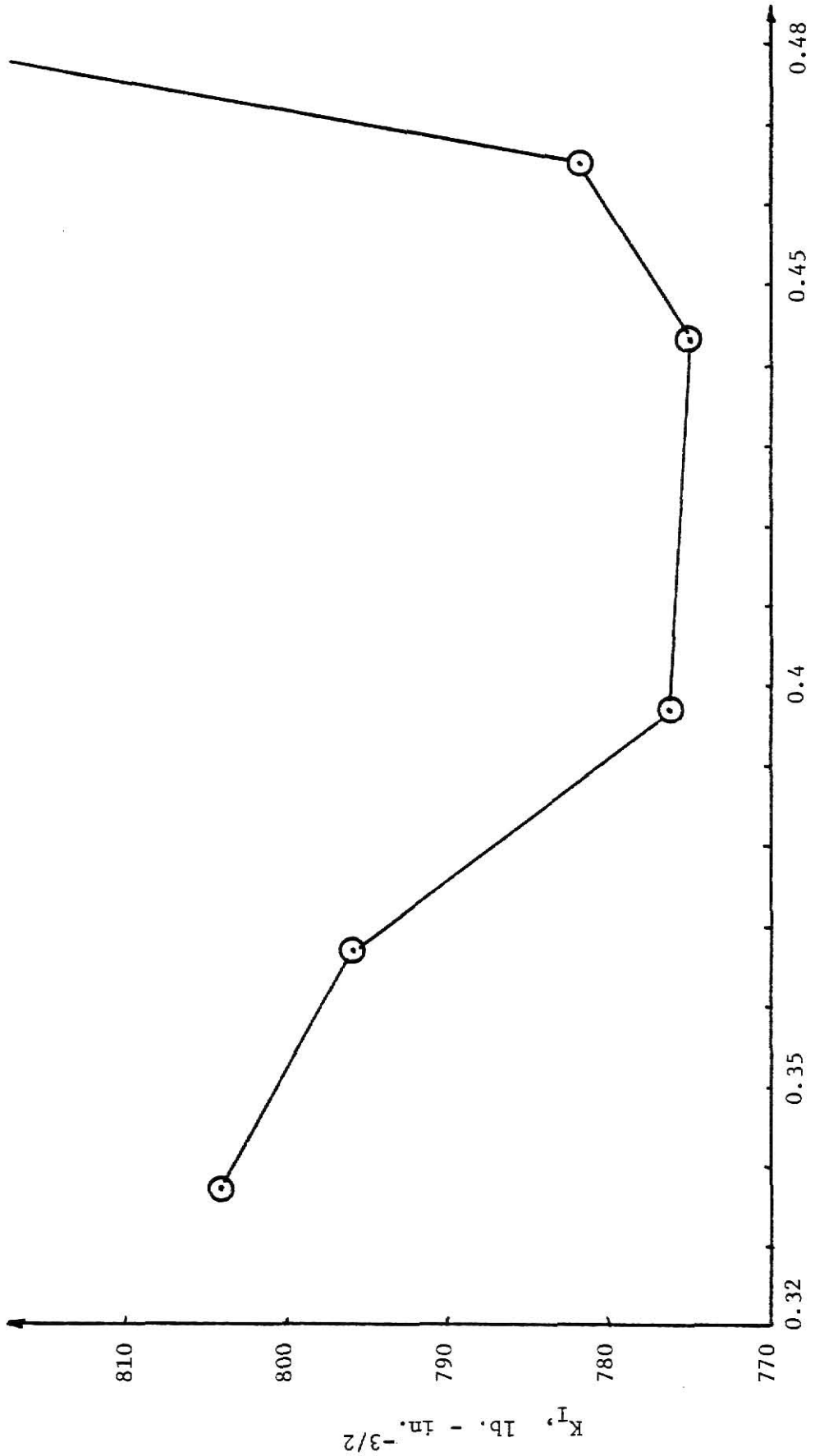

Fig. 4.15 - Stress Intensity V Crack Depth/Beam Depth, (2-A.11), Beam Failed at $\frac{a}{w} = 0.483$, $K_I = 846$ lb. - in.$^{-3/2}$
1 lb. - in.$^{-3/2} = 1.1$ kN - m$^{-3/2}$

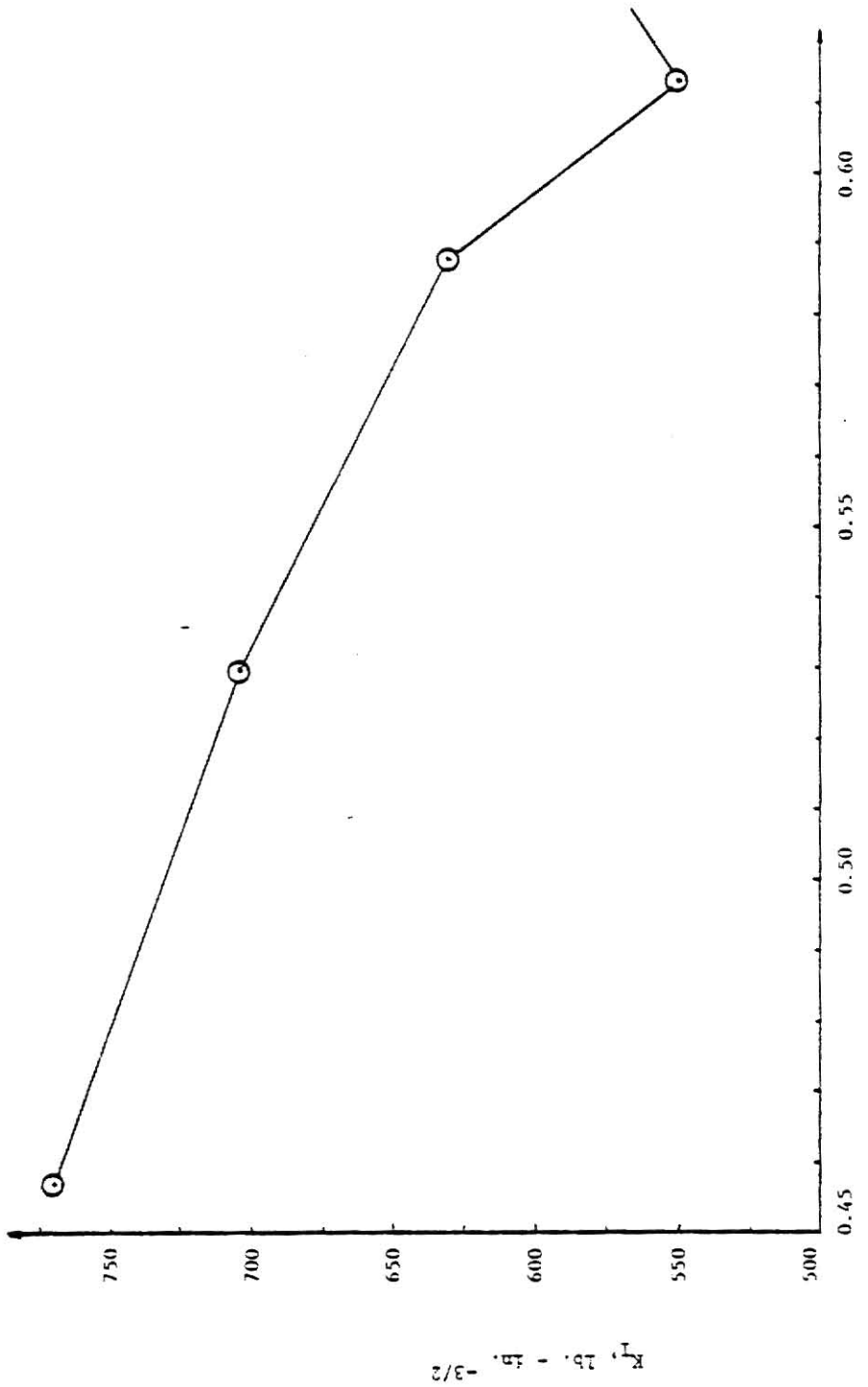

Fig. 4.16 – Stress Intensity (K_I) V Crack Depth/Beam Depth, (3-A.14), Beam Failed at $\frac{a}{w}$ = 0.672, K_I = 648 lb.-in.$^{-3/2}$
1 lb. - in.$^{-3/2}$ = 1.1 kN - m$^{-3/2}$

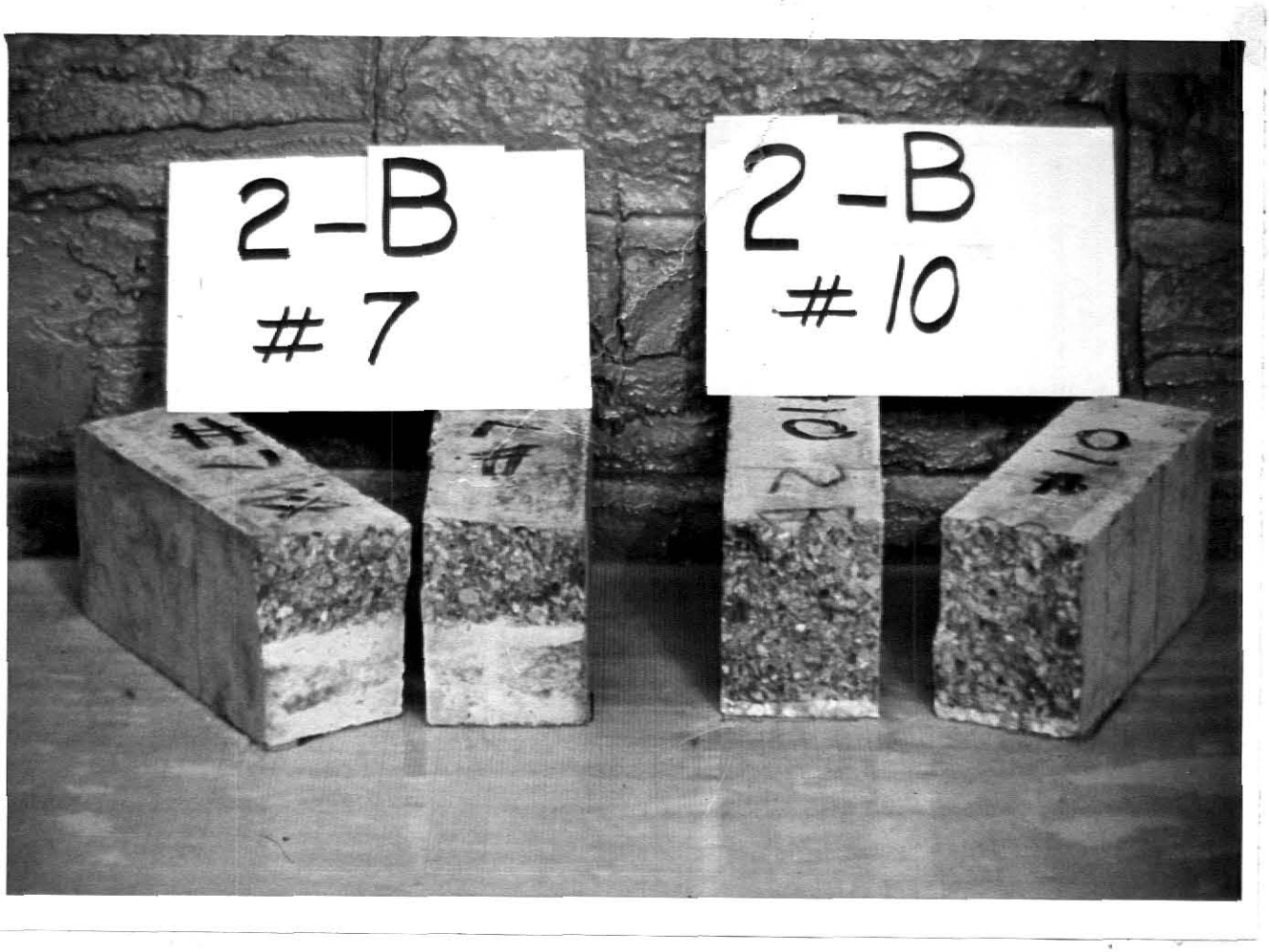

Fig. 4.17

Failure Surfaces for Prenotch (2-B.7) and Precrack (2-B.10) Beams

Table 4.1, Results for beams 1-A (Teflon) with $\frac{a}{w} = 0.3$, Average $f'_c = 2917$ psi

Beam No.	Load, P_{max} (lb.)	Experimental[+] values of a/w	Compliance x 10^{-6} (in./lb.)	Net bending stress, σ_b (psi)	Stress intensity K_I (lb.-in.$^{-3/2}$)
1-A.1	685	0.278	0.824	616.0	661
1-A.2	648	0.218	0.639	496.7	572
1-A.3	635	0.285	0.857	582.2	619
1-A.4	698	0.235	0.692	559.1	632
1-A.5	670	0.280	0.831	605.8	650
1-A.6	674	0.297	0.889	639.3	674
1-A.7	603	0.257	0.764	512.0	564
Average	659	0.264	0.785	573	624.6
Standard Deviation	32.60	0.0288	0.09133		42.69
Coefficient of variation, %	4.95	10.92	11.63		6.84

[+] Experimental values of a/w obtained for compliance calibration curve, Fig. 4-1.

$K_I = P_{max}$ x (value of K_I from K_I $\underline{V}$ a/w curve for unit load, Fig. 4-7)

1 lb. = 4.45 N
1 in. = 25.4 mm.

Table 4·2, Results for beam 1-A (static precrack) with $\frac{a}{w}$ = 0.3, Average f'_c = 2917 psi

Beam No.	Load, P_{max} (lb.)	Experimental+ values of a/w	Compliance x 10^{-6} (in./lb.)	Net bending stress, σ_b (psi)	Stress intensity K_I (lb.-in.$^{-3/2}$)
1-A.10	918	0.296	0.886	868.2	918
1-A.11	848	0.283	0.844	773.2	827
1-A.12	895	0.286	0.865	822.9	873
1-A.13	752	0.384	1.412	929.0	880
1-A.14	862	0.277	0.812	773.0	829
1-A.15	890	0.273	0.811	789.3	854
1-A.16	928	0.255	0.760	783.8	865
Average	870.4	0.293	0.913	819.9	863.7
Standard Deviation	59.39	0.0419	0.224		31.48
Coefficient of variation, %	6.82	14.30	24.52		3.65

+ Experimental values of a/w obtained from compliance calibration curve, Fig. 4.1

$K_I = P_{max}$ x (values of K_I from K_I V a/w curve for unit load, Fig. 4.7)

1 lb. = 4.45 N
1 in. = 25.4 mm.

Table 4.3, Results for beam 2-A (Teflon) with $\frac{a}{w}$ = 0.5, Average f'_c = 3339 psi

Beam No.	Load, P_{max} (lb.)	Experimental+ values of a/w	Compliance x 10^{-6} (in./lb.)	Net bending stress, σ_b (psi)	Stress intensity K_I (lb.-in.$^{-3/2}$)
2-A.1	330	0.490	2.333	594.7	488
2-A.2	300	0.478	2.154	516.1	431
2-A.3	368	0.478	2.154	633.1	528
2-A.4	368	0.482	2.222	642.9	532
2-A.5	294	0.498	2.462	546.9	442
2-A.6	300	0.498	2.462	558.0	451
2-A.7	265	0.518	2.750	534.7	421
Average	317.9	0.492	2.362	575.2	470.4
Standard Deviation	39.11	0.0144	0.215		45.82
Coefficient of variation, %	12.30	2.930	9.105		9.74

+Experimental values of a/w obtained from compliance calibration curve, Fig. 4.2

$K_I = P_{max}$ x (Value of K_I from K_I $\underline{V}$ a/w curve for unit load, Fig. 4.7)

1 lb. = 4.45 N
1 in. = 25.4 mm.

Table 4.4, Results for beams 2-A (static precrack) with $\frac{a}{w}$ = 0.5, Average f'_c = 3339 psi

Beam No.	Load, P_{max} (lb.)	Experimental[+] values of a/w	Compliance x 10^{-6} (in./lb.)	Net bending stress, σ_b (psi)	Stress intensity K_I (lb.-in.$^{-3/2}$)
2-A.10	490	0.557	3.500	1170.4	858
2-A.11	585	0.483	2.250	1025.9	846
2-A.12	572	0.505	2.556	1094.3	878
2-A.13	675	0.415	1.846	924.6	844
2-A.14	575	0.498	2.462	1069.6	864
2-A.15	548	0.500	2.472	1027.5	823
2-A.16	445	0.525	2.895	924.5	721
Average	555.7	0.498	2.569	1033.8	833.4
Standard Deviation	73.44	0.0435	0.519		52.51
Coefficient of variation, %	13.22	8.73	20.22		6.30

[+]Experimental values of a/w obtained from compliance calibration curve, Fig. 4.2

$K_I = P_{max}$ x (value of K_I from K_I $\underline{V}$ a/w curve for unit load, Fig. 4.7)

1 lb. = 4.45 N
1 in. = 25.4 mm.

Table 4.5, Results for beams 3-A (Teflon) with $\frac{a}{w} = 0.7$, Average $f'_c = 3332$ psi

Beam No.	Load, P_{max} (lb.)	Experimental+ values of a/w	Compliance x 10^{-6} (in./lb.)	Net bending stress, σ_b (psi)	Stress intensity K_I (lb.- in.$^{-3/2}$)
3-A.1	85	0.692	12.500	420.0	217
3-A.2	85	0.688	12.000	409.3	215
3-A.3	105	0.670	9.750	452.0	252
3-A.4	83	0.687	11.944	397.1	210
3-A.5	100	0.682	11.111	463.5	248
3-A.6*	98	0.664	9.091	406.9	231
3-A.7	74	0.697	13.333	377.8	191
Average	85.4	0.689	12.178	413.5	216.2
Standard Deviation	9.34	0.00563	0.816		20.535
Coefficient of variation, %	10.94	0.82	6.700		9.50

+Experimental values for a/w obtained from compliance calibration curve, Fig. 4.3

*Data for this beam were not used in calculation of Average, Standard Deviation, and Coefficient of Variation.

$K_I = P_{max}$ x (value of K_I from K_I V a/w curve for unit load, Fig. 4.7)

1 lb. = 4.45 N
1 in. = 25.4 mm.

Table 4.6, Results for beams 3-A (static precrack) with $\frac{a}{w}$ = 0.7, Average f'_c = 3332 psi

Beam No.	Load, P_{max} (lb.)	Experimental[+] values of a/w	Compliance x 10^{-6} (in./lb.)	Net bending stress, σ_b (psi)	Stress intensity K_I (lb.-in.$^{-3/2}$)
3-A.10	150	0.688	12.000	722.3	379
3-A.11	155	0.718	21.176	913.6	424
3-A.12	155	0.719	21.765	920.2	424
3-A.13*	338	0.628	5.714	1144.9	718
3-A.14*	270	0.672	10.000	1176.4	648
3-A.15	157	0.718	21.333	925.4	429
3-A.16	180	0.692	12.400	889.4	459
Average	159.4	0.707	17.735	874.2	423.0
Standard Deviation	11.80	0.0156	5.059		28.59
Coefficient of variation, %	7.40	2.20	28.53		6.76

[+]Experimental values of a/w obtained from compliance calibration curve, Fig. 4.3

*Data for this beam were not used in calculations of Average, Standard Deviation, and coefficient of variation.

$K_I = P_{max}$ x (value of K_I from K_I V a/w curve for unit load, Fig. 4.7).

1 lb. = 4.45 N
1 in. = 25.4 mm.

Table 4.7, Results for beams 1-B (Teflon) with $\frac{a}{w}$ = 0.3, Average f'_c = 6605 psi

Beam No.	Load, P_{max} (lb.)	Experimental[+] values of a/w	Compliance x 10^{-6} (in./lb.)	Net bending stress, σ_b (psi)	Stress intensity K_I (lb.-in.$^{-3/2}$)
1-B.1*	1150	0.250	0.436	606.9	805
1-B.2	1170	0.285	0.511	679.4	848
1-B.3*	1240	0.255	0.442	663.3	868
1-B.4	1230	0.270	0.482	685.2	877
1-B.5	1230	0.275	0.479	694.7	879
1-B.6	1120	0.285	0.507	650.4	812
1-B.7*	1300	0.265	0.471	714.4	923
Average	1187.5	0.279	0.495	677.4	854.0
Standard Deviation	53.15	0.0075	0.01658		31.38
Coefficient of Variation, %	4.48	2.688	3.35		3.67

[+]Experimental values of a/w obtained from compliance calibration curve Fig. 4.4.

*Data for this beam were not used in calculations of Average, Standard Deviation, and Coefficient of Variation.

$K_I = P_{max}$ x (value of K_I from K_I $\underline{V}$ a/w curve for unit load, Fig. 4.8).

1 lb. = 4.45 N
1 in. = 25.4 mm.

Table 4.8, Results for beams 1-B (Static Pre-crack) with $\frac{a}{w}$ = 0.3, Average f'_c = 6605 psi

Beam No.	Load, P_{Max} (lb.)	Experimental[+] values of a/w	Compliance x 10^{-6} (in./lb.)	Net bending stress, σ_b (psi)	Stress intensity K_I (lb.-in.$^{-3/2}$)
1-B.10	1710	0.280	0.500	979.3	1240
1-B.11	1565	0.290	0.516	921.7	1135
1-B.12	1515	0.270	0.488	844.0	1083
1-B.13	1580	0.270	0.482	880.2	1130
1-B.14	1610	0.270	0.481	896.9	1151
1-B.15	1500	0.275	0.493	847.2	1080
1-B.16	1535	0.275	0.492	867.0	1105
Average	1574	0.276	0.493	890.9	1132
Standard Deviation	71.16	0.00732	0.012		54.58
Coefficient of Variation, %	4.52	2.652	2.441		4.82

[+]Experimental values of a/w obtained from compliance calibration curve, Fig. 4.4.

$K_I = P_{max}$ x (value of I_I from K_I $\underline{V}$ a/w curve for unit load, Fig. 4.8)

1 lb. = 4.45 N
1 in. = 25.4 mm.

Table 4.9, Results for beams 2-B (Teflon) with $\frac{a}{w}$ = 0.5, Average f'_c = 6646 psi

Beam No.	Load, P_{max} (lb.)	Experimental[+] values of a/w	Compliance x 10^{-6} (in./lb.)	Net bending stress, σ_b (psi)	Stress intensity K_I (lb.-in.$^{-3/2}$)
2-B.1	515	0.537	1.781	713.2	605
2-B.2	480	0.527	1.667	636.9	552
2-B.3	470	0.537	1.762	650.9	552
2-B.4*	550	0.510	1.500	680.1	605
2-B.5*	580	0.513	1.529	726.0	638
2-B.6*	498	0.510	1.500	615.8	548
2-B.7	595	0.520	1.606	766.7	669
Average	515	0.530	1.704	691.9	594.5
Standard Deviation	56.716	0.0083	0.0822		55.597
Coefficient of Variation, %	11.01	1.566	4.823		9.35

[+]Experimental values of a/w obtained from compliance calibration curve, Fig. 4.5.

*Data for this beam were not used in calculations of Average, Standard Deviation, and Coefficient of Variation.

$K_I = P_{max}$ x (value of K_I from K_I V a/w curve for unit load, Fig. 4.8).

1 lb. = 4.45 N
1 in. = 25.4 mm.

Table 4.10, Results for beams 2-B (Static Pre-crack) with $\frac{a}{w} = 0.5$, Average $f'_c = 6646$ psi

Beam No.	Load, P_{max} (lb.)	Experimental[+] values of a/w	Compliance x 10^{-6} (in./lb.)	Net bending stress, σ_b (psi)	Stress intensity K_I (lb.-in.$^{-3/2}$)
2-B.10	930	0.530	1.690	1249.9	1074
2-B.11*	860	0.557	1.917	1301.0	1062
2-B.12*	1090	0.495	1.382	1268.9	1156
2-B.13	940	0.522	1.615	1221.4	1058
2-B.14	920	0.540	1.800	1290.8	1093
2-B.15	820	0.543	1.815	1165.6	976
2-B.16	840	0.535	1.758	1153.3	987
Average	890	0.534	1.736	1216.2	1037.6
Standard Deviation	55.68	0.0083	0.083		52.833
Coefficient of Variation, %	6.26	1.56	4.78		5.09

[+]Experimental values of a/w obtained from compliance calibration curve, Fig. 4.5.

*Data for this beam were not used in calculations of Average, Standard Deviation, and Coefficient of Variation.

$K_I = P_{max}$ x (value of K_I from K_I V a/w curve for unit load, Fig. 4.8)

1 lb. = 4.45 N
1 in. = 25.4 mm.

Table 4.11, Results for beams 3-B (Teflon) with $\frac{a}{w}$ = 0.7, Average f'_c = 6024 psi

Beam No.	Load, P_{max} (lb.)	Experimental[+] values of a/w	Compliance x 10^{-6} (in./lb.)	Net bending stress, σ_b (psi)	Stress intensity K_I (lb.-in.$^{-3/2}$)
3-B.1	190	0.731	6.944	779.5	313.5
3-B.2	210	0.726	6.667	830.4	388.5
3-B.3	200	0.705	5.682	682.3	350.0
3-B.4	185	0.710	6.905	653.1	324.7
3-B.5	180	0.726	6.667	711.8	333.0
3-B.6	200	0.713	6.042	720.8	356.0
3-B.7[*]	218	0.672	4.483	601.6	354.3
Average	194.2	0.719	6.485	729.7	344.3
Standard Deviation	11.143	0.0105	0.509		26.771
Coefficient of Variation, %	5.74	1.46	7.846		7.78

[+]Experimental values of a/w obtained from compliance calibration curve, Fig. 4.6.

[*]Data for this beam were not used in calculations of Average, Standard Deviation, and Coefficient of Variation.

$K_I = P_{max}$ x (value of K_I from K_I V a/w curve for unit load, Fig. 4.8).

1 lb. = 4.45 N
1 in. = 25.4 mm.

Table 4.12, Results for beams 3-B (Static Pre-crack) with $\frac{a}{w}$ = 0.7, Average f'_c = 6024 psi

Beam No.	Load, P_{max} (lb.)	Experimental[+] values of a/w	Compliance x 10^{-6} (in./lb.)	Net bending stress, σ_b (psi)	Stress intensity K_I (lb.-in.$^{-3/2}$)
3-B.10*	F	A	I	L	E	D
3-B.11*	F	A	I	L	E	D
3-B.12	360	0.737	7.333	1545.1	676.8
3-B.13	360	0.742	7.571	1605.6	684.0
3-B.14	420	0.732	7.000	1736.0	782.5
3-B.15	380	0.734	7.125	1594.4	712.5
3-B.16	460	0.722	6.429	1767.0	839.5
Average	396	0.733	7.092	1649.6	739.1
Standard Deviation	43.36	0.0074	0.429		69.98
Coefficient of Variation, %	10.95	1.01	6.051		9.47

[+]Experimental values of a/w obtained from compliance calibration curve, Fig. 4.6.

*Data for this beam were not used in calculations of Average, Standard Deviation, and Coefficient of Variation.

$K_I = P_{max}$ x (value of K_I from K_I $\underline{V}$ a/w curve for unit load, Fig. 4.8).

1 lb. = 4.45 N
1 in. = 25.4 mm.

Table 4.13, Summarized a/w and stress intensity values for Mix A

	a/w		K_I (lb. - in.$^{-3/2}$)	
MARK	AVG.	COEF. (%)	AVG.	COEF. (%)
1-T*	0.264	10.9	625	6.8
1-N**	0.293	14.3	864	3.6
2-T	0.492	2.9	470	9.7
2-N	0.498	8.7	833	6.3
3-T	0.689	0.8	216	9.5
3-N	0.707	2.2	423	6.8

* Beams with teflon

** Beams without teflon

Table 4.14, Summarized a/w and stress intensity values for Mix B

	a/w		K_I (lb. - in.$^{-3/2}$)	
MARK	AVG.	COEF. (%)	AVG.	COEF. (%)
1-T*	0.279	2.7	854	3.7
1-N**	0.276	2.6	1132	4.8
2-T	0.530	1.6	595	9.4
2-N	0.534	1.6	1038	5.1
3-T	0.719	1.5	344	7.8
3-N	0.733	1.0	739	9.5

* Beams with teflon

** Beams without teflon

Chapter 5

SUMMARY AND CONCLUSIONS

The experimental investigation described in this thesis may be summarized as follows:

1. In all cases the naturally-cracked beams yield higher failure loads, stress intensity values, and bending stresses than notched beams with the same crack length.
2. The average K_I values for precracked beams were approximately 38%, 77%, and 96% in Mix A and 33%, 75%, and 115% in Mix B, greater than for notched beams for crack depth ratios of 0.3, 0.5, and 0.7 respectively.
3. The failure surface appearance in the region beyond the initial crack for the beams with notches was identical to that for beams which were pre-cracked. For the pre-cracked beams, there was no difference in appearance between the surface of the initial crack and the final failure surface. The crack surface was frequently planar but in a number of cases it was also skewed.
4. True fracture toughness can not be obtained with notched beams. Pre-cracked beams or some correlation between results obtained for notched versus pre-cracked beams must be used (i.e. equation 1).
5. Excellent repeatability of results was obtained.

REFERENCES

1. Brown, W. F., Jr. and Srawley, J. E., "Plain Strain Crack Toughness Testing of High Strength Metallic Materials," STP410, ASTM, 1967.

2. Hillemeier, B. and Hilsdorf, H. K., "Fracture Mechanics Studies on Concrete Compounds," Cement and Concrete Research, Vol. 7, 1977.

3. Huang, C. M., Swartz, S. E., and Hu, K. K., "On the Experimental and Numerical Analysis of Fracture Toughness of Plain Concrete Beams," presented at the ASTM symposium on Fracture Mechanics Methods for Ceramics, Rocks, and Concrete, Chicago, Il., June 23-24, 1980.

4. Naus, Don J. and Lott, James L., "Fracture Toughness of Portland Cement Concretes," Journal of the American Concrete Institute, Vol. 66, No. 6, June 1969.

5. Schmidt, R. A., "Fracture Toughness Testing of Limestone," Experimental Mechanics, Vol. 16, No. 5, May 1976.

6. Swartz, Stuart E., Hu, Kuo-Kuang, and Jones, Gary L., "Compliance Monitoring of Crack Growth in Concrete," Journal of the Engineering Mechanics Division, ASCE, Vol. 104, No. EM4, Aug., 1978.

7. Swartz, Stuart E., Hu, K. K., and Huang, James, "Displacement Gage Mount for Concrete Beams," Experimental Techniques, Society for Experimental Stress Analysis, Vol. 4, No. 2, 1980.

8. Swartz, S. E., Huang, C. M. James, and Hu, K. K., "Crack Growth and Fracture in Plain Concrete-Static Versus Fatigue Loading," presented at the symposium on Recent Research in Fatigue on Concrete Structures, Fall Convention, American Concrete Institute San Juan, Puerto Rico, Sept. 21-26, 1980.

STRESS INTENSITY VALUES FOR PRENOTCHED AND PRECRACKED, PLAIN CONCRETE BEAMS

by

Mojtaba Fartash

B.S., University of Missouri - Columbia, 1979

AN ABSTRACT OF A MASTER'S THESIS

submitted in partial fulfillment of

the requirements for the degree of

MASTER OF SCIENCE

Department of Civil Engineering

KANSAS STATE UNIVERSITY
Manhattan, Kansas

1981

ABSTRACT

A series of experiments conducted to compare the behavior of beams with notches to those with natural cracks has recently been completed. A total of 42 beams with notches formed by casting teflon strips into the concrete were tested to failure. A companion series of 42 beams were statically precracked following the procedure described in Reference 3 of the report. The ranges of crack depth to beam depth varied from 0.3 to 0.7 (nominally). Two strengths of concrete were used denoted Mix A and Mix B and the 3 in. x 4 in. x 15 in. (span) beams were tested in 3 point or 4 point bending.

Results are as follows:

1. In all cases the naturally - cracked beams yielded higher failure loads and stress-intensity values than notched beams with the same crack length.
2. The average K_I values for precracked beams were approximately 38%, 77%, and 96% in Mix A and 33%, 75%, and 115% in Mix B, greater than for notched beams for crack depth ratios of 0.3, 0.5, and 0.7 respectively.
3. The failure surface appearance in the region beyond the initial crack for the beams with notches was identical to that for beams which were pre-cracked. For the pre-cracked beams, there was no difference in appearance between the surface of the initial crack and the final failure surface. The crack surface was frequently planar but in a number of cases was also skewed.

4. True fracture toughness can not be obtained with notched beams. Precracked beams or some correlation between results obtained for notched versus precracked beams must be used.
5. Excellent repeatability of results was obtained.